Multiple Sulfur Isotope Systematics of Geothermal Fluids at Krafla, NE Iceland, and the Source and Reactions of Sulfur in Volcanic Geothermal Systems

Jóhann Gunnarsson Robin

Faculty of Earth Sciences
University of Iceland
2015

Multiple Sulfur Isotope Systematics of Geothermal Fluids at Krafla, NE Iceland, and the Source and Reactions of Sulfur in Volcanic Geothermal Systems

Jóhann Gunnarsson Robin

60 ECTS thesis submitted in partial fulfillment of a
Magister Scientiarum degree in geology

Advisors
Andri Stefánsson
Nicole Keller

Faculty Representative
Stefán Arnórsson

Faculty of Earth Sciences
School of Engineering and Natural Sciences
University of Iceland
Reykjavik, January 2015

Multiple Sulfur Isotope Systematics of Geothermal Fluids at Krafla, NE Iceland, and the Source and Reactions of Sulfur in Volcanic Geothermal Systems
Multiple S-Isotope Systematics of Geothermal Fluids
60 ECTS thesis submitted in partial fulfillment of a *Magister Scientiarum* degree in geology

Faculty of Earth Sciences
School of Engineering and Natural Sciences
University of Iceland
Sturlugata 7
101, Reykjavik
Iceland

Telephone: 525 4600

Bibliographic information:
Jóhann Gunnarsson Robin, 2015, *Multiple Sulfur Isotope Systematics of Geothermal Fluids at Krafla, NE Iceland, and the Source and Reactions of Sulfur in Volcanic Geothermal Systems*, Master's thesis, Faculty of Earth Sciences, University of Iceland, pp. 36.

Printing: Háskólaprent
Reykjavik, Iceland, January 2015

Abstract

Multiple sulfur isotope systematics of geothermal fluids at Krafla NE Iceland were studied in order to determine the source and reactions of sulfur in the systems. Fluid temperatures ranged from 192 to 437°C with liquid water, vapor and superheated vapor being present in the reservoir. Dissolved sulfide (ΣS^{-II}) and SO_4 predominated in the water phase with trace concentrations of S_2O_3 whereas H_2S was the only species observed in the vapor phase. The reconstructed sulfur isotope ratios of the reservoir fluids based on samples collected at surface from two-phase well discharges indicate that $\delta^{34}S$ and $\Delta^{33}S$ of sulfide in the reservoir water and vapor are in the ranges of -1.45 to +1.13 ‰ and -0.017 to -0.001 ‰ whereas the $\delta^{34}S$ and $\Delta^{33}S$ ranges of sulfate are significantly different or +3.40 to +13.37 ‰ and 0.000 to -0.036 ‰, respectively. Depressurisation boiling upon fluid ascent and progressive fluid-rock interaction and sulfide mineral (pyrite) formation results in the liquid phase becoming progressively isotopically lighter both with respect to $\delta^{34}S$ and $\Delta^{33}S$. In contrast, the H_2S in the vapor phase and pyrite formed become isotopically heavier. The observed $\Delta^{33}S$ and $\delta^{34}S$ systematics for geothermal fluids at Krafla suggest that the source of sulfides in the fluids is the basaltic magma, either through degassing or upon dissolution of unaltered basalts. At high temperatures, insignificant SO_4 is observed in the fluids but below ~230°C significant concentrations of SO_4 are observed, the source considered to be H_2S oxidation. Sulfate originated from the meteoric source water of the geothermal fluids is, however, considered to be negligible. The key factors controlling the multiple sulfur isotope systematics of geothermal fluids are the isotope composition of the source material, and isotope fractionation associated with aqueous and vapor speciation and how these change as a function of processes occurring in the system such as boiling, oxidation and fluid-rock interaction.

Útdráttur

Stöðugar brennisteinssamsætur í jarðhitavökva frá Kröflu voru athugaðar til að greina uppruna og hvarfleiðir brennisteins í kerfinu. Hitastig jarðvitavökvans var á bilinu 192 til 437°C og var til staðar í vökvaham, gufuham og sem yfirhituð gufa. Uppleyst súlfíð (ΣS^{-II}) og súlfat (SO_4) eru ríkjandi í vatnsfasanum en snefilmagn S_2O_3 er einnig til staðar. Í gufufasanum var H_2S eina greinda efnasambandið. Hlutfall brennisteinssamsætanna í forðavökva var reiknað út frá mældum hlutföllum í yfirborðssýnum og benti reiknað hlutfall til þess að $\delta^{34}S$ og $\Delta^{33}S$ súlfíða í forðavökva séu á bilinu -1.45 til +1.13 ‰ og -0.017 til -0.001 ‰, en $\delta^{34}S$ og $\Delta^{33}S$ súlfats séu hinsvegar á bilinu +3.40 til +13.37 ‰ og 0.000 til -0.036 ‰. Suða vegna þrýstifalls og samspil bergs og vatns við myndun pýríts valda því að samsætuhlutföll vatnsfasans, $\delta^{34}S$ og $\Delta^{33}S$, lækka. $\delta^{34}S$ og $\Delta^{33}S$ H_2S í gufufasanum og í pýrítinu hækka hinsvegar eftir því sem ferlið gengur lengra. Reiknuð $\Delta^{33}S$ og $\delta^{34}S$ í jarðhitavökva Kröflu benda til þess að súlfíð í vökvanum séu upprunin í basaltkviku, annaðhvort með afgösun kviku eða með uppleysingu á óveðruðu basalti. Við háan hita er styrkur SO_4 í vökvanum óverulegur en undir ~230°C eykst styrkur þess verulega og er talinn stafa af oxun H_2S. Súlfat úr regnvatni er hinsvegar talið óverulegur hluti vökvans. Þeir meginþættir sem stýra hlutföllum brennisteinssamsæta í jarðhitavökva eru því annarsvegar upprunaleg hlutföll í uppsprettu brennisteinsins og hinsvegar aðgreining samsæta í samspili við samsetningu brennisteinssambanda í vökvanum og hvernig hún þróast sem fall af þeim ferlum sem eiga sér stað í kerfinu, svo sem suðu, oxun og samspil vökvans við berg.

Table of Contents

List of Figures

List of Tables

Acknowledgements

I'm grateful to my supervisor, Andri Stefánsson, for letting me work with him on this project and encouraging me to continue when the outlook was dark, as well as countless discussions on the nature of geochemistry. I would like extend gratitude to Nicole Keller for support and teaching me how to do the extractions and advices on various lab subjects and editorial matters, as well as for the many talks we had on the subject.

I don't know how to begin to thank Eyrún Björgvinsdóttir, for always being there for me, keeping me on track and listening to me agonising.

I'd like to thank my coworkers at Askja, especially Jón Örn Bjarnason for illuminating discussions about WATCH and the thermodynamic properties of wells, Ríkey Kjartansdóttir for extreme moral support, Eydís Salóme Eiríksdóttir and Iwona Galeczka for various discussions and help in the lab. The bunch playing floor hockey kept me amused and moving for most of the first two years, and for that I'm grateful.

I also want to thank a great friend and philosophiser, Sigurður Helgi Oddsson, for our mutual writing support group and various activities unrelated to this work, but nonetheless neccesary.

1 Introduction

Sulfur is among the major components in volcanic geothermal fluids and is found both in the liquid and the vapor phase. Dissolved sulfide (S^{-II}) and sulfate (S^{VI}) predominate in the liquid phase whereas sulfide (S^{-II}) is the predominant form in the vapor phase (e.g. Giggenbach, 1980; Arnórsson et al., 1983; Marini et al., 2011). Additionally, minor sulfur species have been observed including thiosulfate ($S_2O_3^{2-}$), sulfite (SO_3^{2-}), polythionates ($S_nO_6^{2-}$), polysulfides (S_n^{2-}) and dissolved elemental sulfur (S^0) (Xu et al., 1998, 2000; Druschel et al., 2003; Kamyshny et al., 2008; Kaasalainen and Stefánsson, 2011b). The sulfur compounds in geothermal fluids may originate from various sources: the source water like meteoric water or seawater; leached out from a fresh or altered host rock; or originated from magmatic degassing. In seawater and meteoric water, sulfur is predominantly present as sulfate, whereas sulfate and sulfides may both be present in the host rock depending on the formation conditions while sulfur dioxide is the stable form of sulfur in magmatic gas (Marini et al., 2011).

The sources and reactions of sulfur compounds in volcanic geothermal fluids have mainly been approached using $\delta^{34}S$ systematics and equilibrium thermodynamics for fluid species and fluid-rock interaction. It is generally accepted that the concentrations of major components including sulfur compounds is controlled by near equilibrium between the fluids and the secondary minerals within the reservoir (Giggenbach, 1980, 1981; Arnórsson et al., 1983). However, for redox sensitive compounds like sulfur this may not be the case (e.g. Stefánsson and Arnórsson, 2002). With respect to sulfur isotope ratios these have also been reported to be at disequilibrium at temperatures as high as 200-300°C (e.g. Ohmoto and Lasaga, 1982).

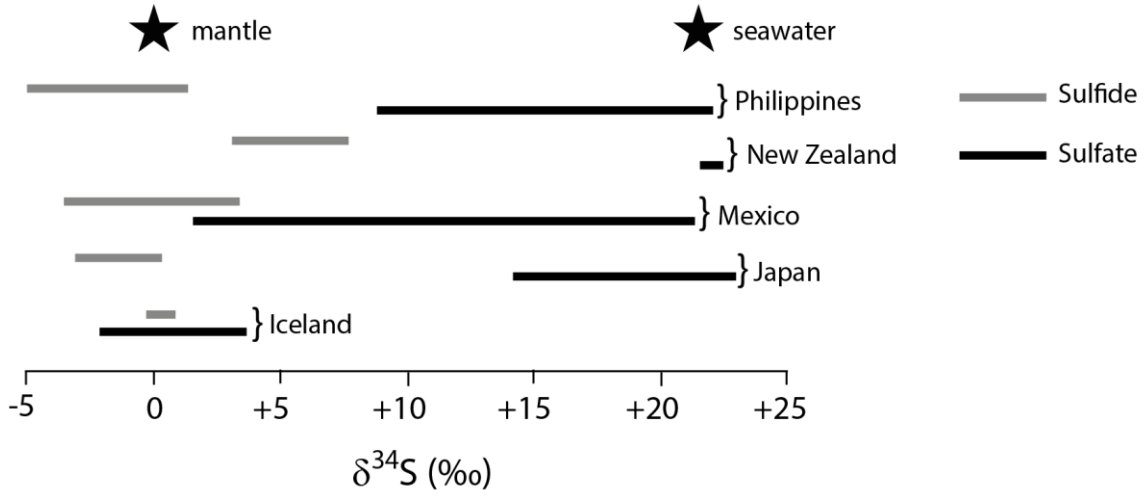

Figure 1 Distribution of $\delta^{34}S$ ratios in geothermal fluids (water and vapor) from various locations in the world. Based on literature values reported by Sakai et al. (1980), Sakai (1983), Robinson (1987), Giggenbach (1992), Matsuda et al. (2005), Bayon and Ferrer (2005), González-P. et al. (2005) and Marini et al. (2011).

Spare data exist for $\delta^{34}S$ ratios of volcanic geothermal fluids and almost none are available for multiple sulfur isotope ratios. Based on available data the $\delta^{34}S$ ratios for sulfide in the water and vapor phase range from -4.4 to +7.9 ‰ whereas dissolved sulfate ratios are between -2.0 to +23.1 ‰ (Fig. 1) (Sakai et al., 1980, Sakai, 1983; Robinson, 1987; Giggenbach, 1992; Matsuda et al., 2005; Bayon and Ferrer, 2005; González-P. et al., 2005). For fluids at convergent plate boundaries, the sulfate values are generally heavier and approach that of seawater whereas the few values at divergent plate boundaries are similar to the sulfide ratios. Based on these findings it has been concluded that the source of sulfide and sulfate may be mantle and seawater in most cases and the variations in sulfur isotope ratios related to various processes including reduction of sulfate, oxidation of sulfide, formation of secondary sulfides and sulfates and SO_2 disproportionation forming H_2S and SO_4 (e.g. Sakai et al., 1980; Bayon and Ferre, 2005; Marini et al., 2011). However, there are also other processes that may be important in affecting sulfur isotope ratios in geothermal fluids, namely aqueous speciation, fluid phase relations like boiling, as well as progressive fluid-rock interaction.

Multiple sulfur isotope systematics provide a useful tool to trace some of these processes including boiling and phase separation, progressive water-rock interaction and secondary mineral formation, oxidation and reduction of various sulfur species and fluid mixing and how sulfur fluid speciation is linked to these processes acting within the volcanic system and their effects on sulfur isotope ratios. The purpose of this study was to investigate the sulfur isotope systematics in volcanic geothermal fluids fed by meteoric water on divergent plate boundaries. For this purpose samples of vapor and liquid from two-phase well discharges at surface were sampled and analysed for sulfur isotopes of sulfide in the vapor phase and sulfide and sulfate in the liquid phase. Using geochemical modelling, the sulfur isotope content of the reservoir was assessed as well as sulfur isotope systematics upon fluid-fluid (boiling) and fluid-rock interaction. In this way, the source and reactions of sulfur in the geothermal fluids were traced.

2 Methods

2.1 Sampling and analysis

Samples of two-phase geothermal well discharges at Krafla geothermal system, NE Iceland, were collected and analysed for major elemental compositions and multiple sulfur isotope ratios.

The liquid and vapor phases were separated at the wellhead using a Webre separator (Fig. 2). Vapor samples were collected into evacuated gas bulbs containing 5-10 ml 50 % w/v KOH. The concentrations of CO_2 and H_2S in the vapor condensate were determined by modified alkalinity titration (Stefánsson et al., 2007) and a precipitation titration method using Hg-acetate and dithizone indicator (Arnórsson et al., 2006), respectively. The non-condensable gases including H_2, N_2, Ar and CH_4 were analysed by gas chromatography (PerkinElmer-ARNEL 4019 Analyzer).

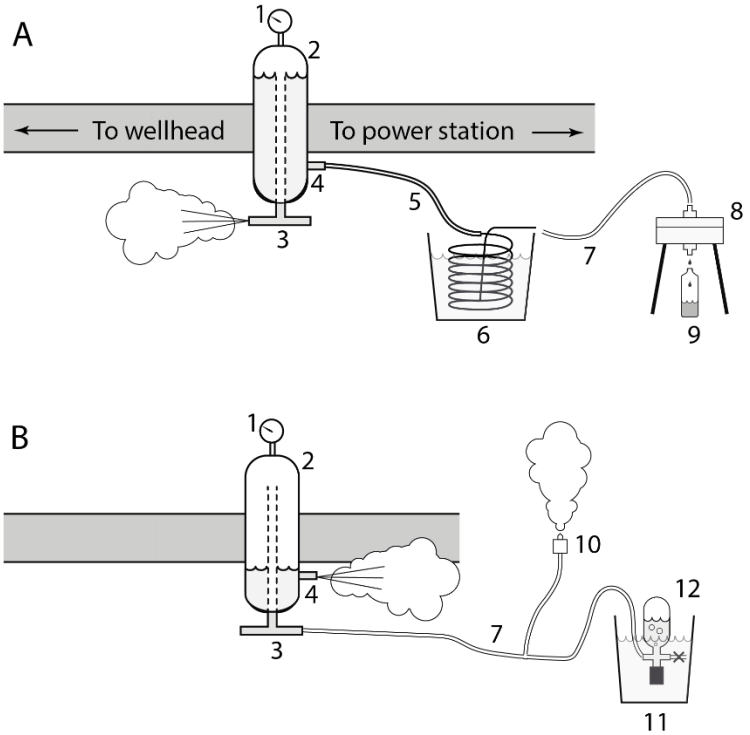

Figure 2 Equipment for the sampling of water (A) and steam (B) from a wet-steam well discharge using a Webre steam separator. (1) Pressure gauge. (2) Webre steam separator. (3) Steam outlet valve. (4) Water outlet valve. (5) Steel-clad Teflon tubing. (6) Bucket with cold water and cooling coil of stainless steel. (7) ¼" diameter thick-walled silicone tubing, connected to the filter holder. (8) Teflon filter holder with 20 cm diameter 0.2 µm filter membrane. (9) Sample bottle. (10) One-way atmospheric valve. (11) Bucket with cold water. (12) Gas sampling bulb 125–250 ml. Figure reproduced and modified for this study from Arnórsson et al. (2006).

The liquid phase samples were cooled down using a stainless steel spiral that was connected to the Webre separator and filtered through 0.2 μm filters (cellulose acetate) into polypropylene and amber glass bottles. Samples for major cation analysis were acidified with 0.5 ml concentrated HNO_3 (Suprapur, Merck) per 100 ml sample and determined using ICP-OES (Spectro Ceros Vision). Two samples for major anion analysis were collected, one not further treated for F and Cl determination and another to which 2 % Zn-acetate solution was added for SO_4 analysis. All anion analyses were carried out using ion chromatography (Dionex ICS-2000). Samples for determination of CO_2 were collected into amber glass bottles and analysed using the aforementioned modified alkalinity titration (Stefánsson et al., 2007). Dissolved H_2S was titrated on-site using the previously described method (Arnórsson et al., 2006). The pH was analysed on-site and in-line within a few seconds of sampling at ~20°C using a flow-through pH cell.

2.2 Sulfur isotope sampling and analysis

Samples of water and vapor for sulfur isotope analysis were collected using a Webre separator. Liquid samples were filtered through 0.2 μm filters (cellulose acetate) into 1 l polypropylene bottles to which 10 ml of 2 % Zn-acetate were added to precipitate H_2S as ZnS solids. Vapor samples were collected into gas-bulbs containing 10-15 ml 50 % w/v KOH and 5 ml 2 % Zn-acetate to precipitate H_2S as ZnS. The ZnS solids for both liquid and vapor samples were filtered through a 0.2 μm filter and the solids collected from the filter paper. The filtered solution from the water phase sample was also collected, to which 5 ml $BaCl_2$ and 1 ml 1 M HCl was added in order to precipitate SO_4 as $BaSO_4$. The solid $BaSO_4$ was subsequently filtered off using 0.2 μm filter and the solids collected from the filter paper.

Extraction and purification of sulfide and sulfate samples were carried out in the following way. The ZnS solids were dissolved in 6 N HCl and flushed with a N_2 gas flow and the evolved H_2S gas was precipitated, first as ZnS in 50 ml of Zn-acetate (Fig. 3), and then as Ag_2S by adding 5 ml $AgNO_3$ to the solution. The Ag_2S was then cleaned in deionized water and dried at 80°C (Alt and Shanks, 1998, with modifications). To obtain the sulfur isotope composition of sulfate the $BaSO_4$ precipitate was dried and reduced to H_2S using the Thode reagent (Thode et al., 1961). The H_2S produced was then flushed through the extraction line with a N_2 gas flow and precipitated as Ag_2S in the Zn-acetate, cleaned in deionized water and dried at 80°C (Fig. 4).

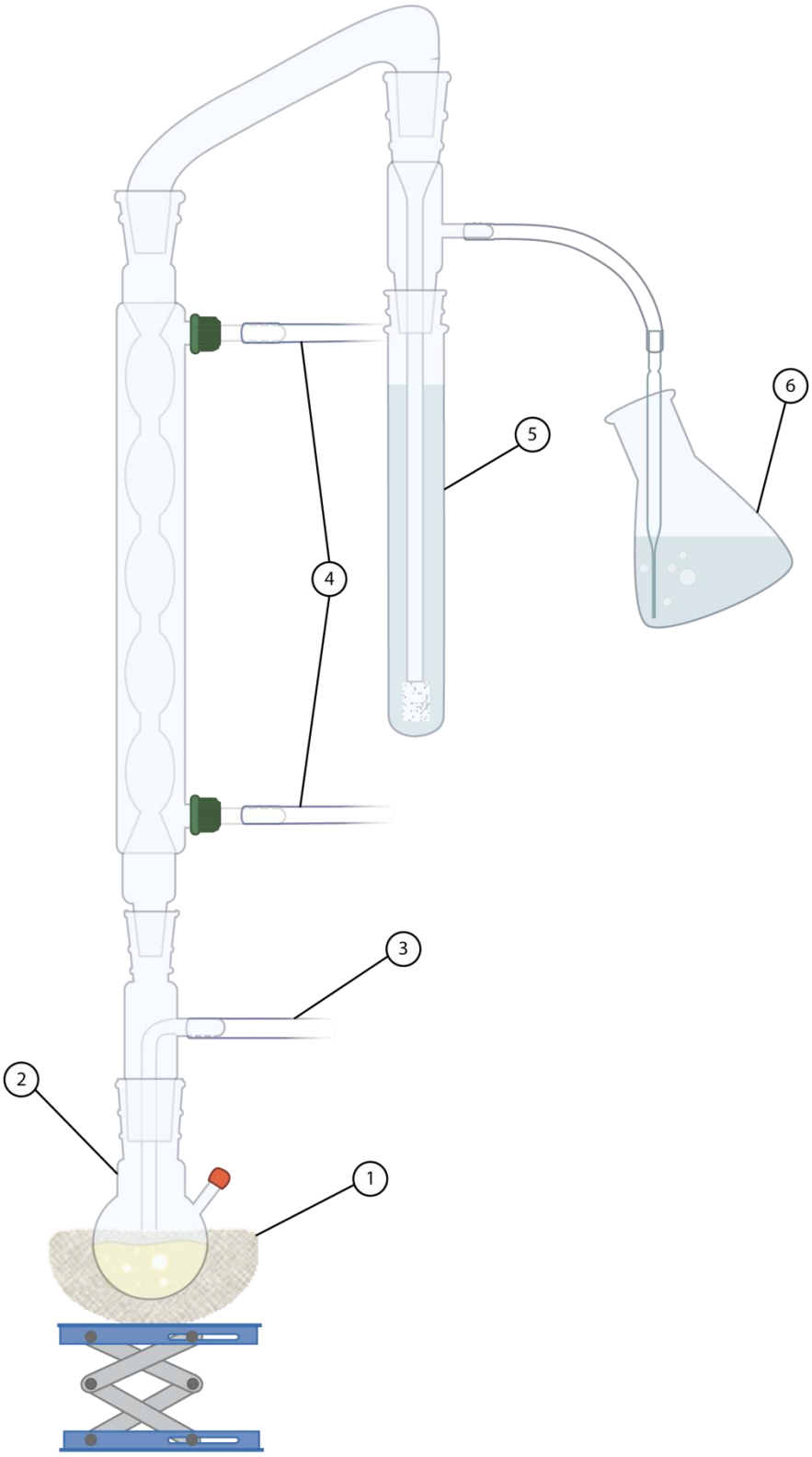

Figure 3 The extraction line setup used to extract sulfur from sulfide samples. (1) Heating mantle. (2) Round flask containing ca.15 mg sample and 30 ml 6 N HCl. (3) N_2 flow from regulator. (4) Cooling water flowing in the condenser. (5) DI water trap. (6) Erlenmeyer flask containing ca. 50 ml Zn-acetate.

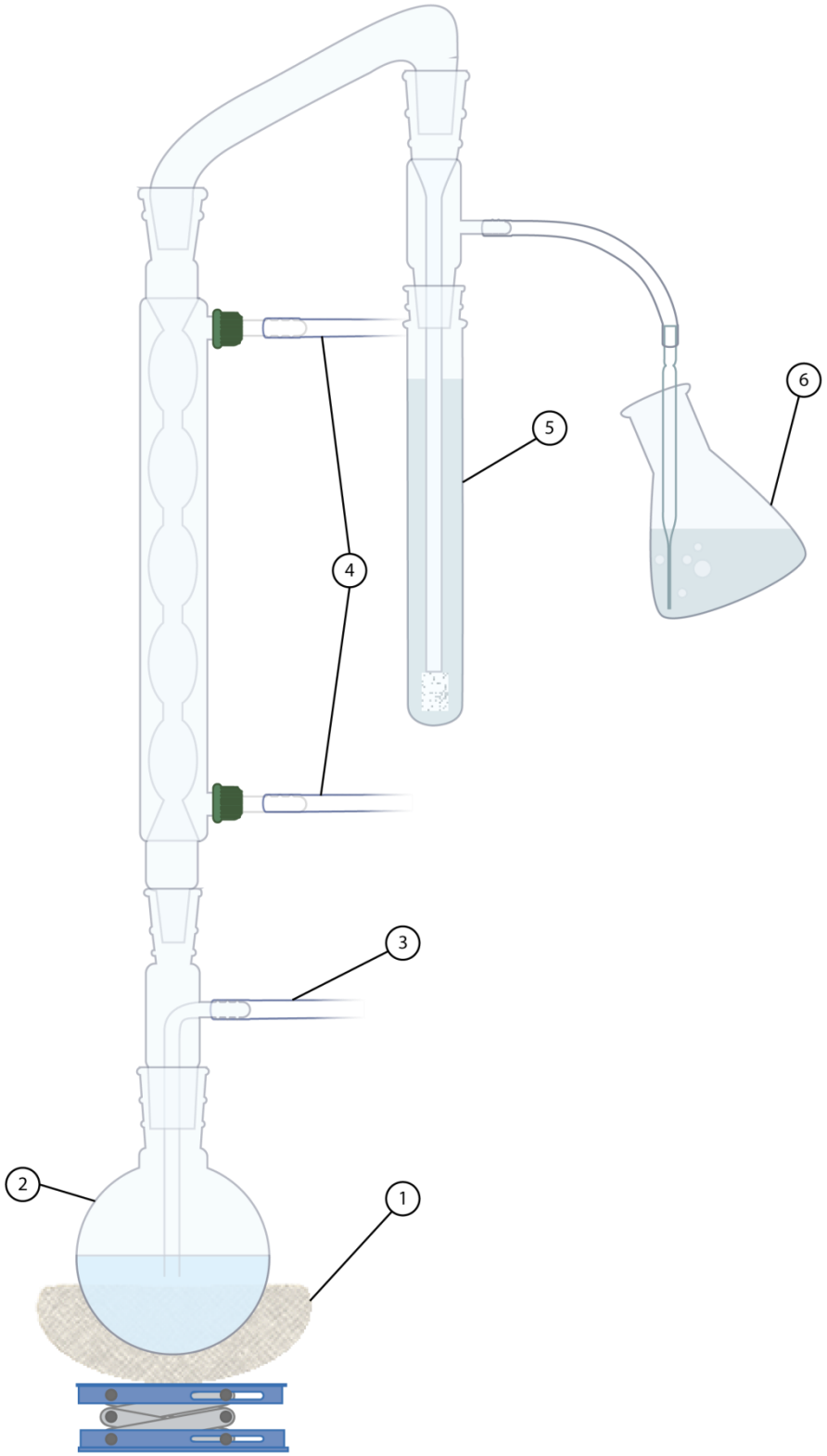

Figure 4 The extraction line setup used to extract sulfur from sulfate samples. (1) Heating mantle. (2) Round flask containing ca. 10 mg sample and 40 ml Thode solution. (3) N_2 flow from regulator. (4) Cooling water flowing in the condenser. (5) DI water trap. (6) Erlenmeyer flask containing ca. 50 ml Zn-acetate.

Sulfur isotope ratios were analysed according to the method described by Ono et al. (2006, 2012). Approximately 2 mg of Ag_2S powder were reacted with elemental fluorine at 300°C for > 6 hours to produce SF_6. The SF_6 was purified by a gas chromatography system equipped with two columns, molesieve 5 Å and HayesepQ, followed by analyses by a Thermoelectron MAT 253 isotope ratio mass spectrometer (Fig. 5). Replicate analysis (n = 28) of IAEA-S-1 reference material yield a standard deviation of 2σ 0.26 ‰, 0.014 ‰ and 0.19 ‰ for $\delta^{34}S$, $\Delta^{33}S$ and $\Delta^{36}S$ (Ono et al., 2012).

Sulfur isotope ratios are reported using the conventional notation,

$$\delta^x S = \left(\frac{\left({}^xS/{}^{32}S \right)_{sample}}{\left({}^xS/{}^{32}S \right)_{VCDT}} - 1 \right) \times 1000 \quad (1)$$

where x = 33, 34 and 36 and VCDT is the Vienna-Cañon Diablo Troilite reference material. The multiple sulfur isotope ratios defined as Δ^xS are defined by,

$$\Delta^{33}S = \delta^{33}S - {}^{33}\theta\delta^{34}S \quad (2)$$

Additionally, one can define

$$\Delta^{36}S = \delta^{36}S - {}^{36}\theta\delta^{34}S \quad (3)$$

As pointed out by Ono et al. (2006) the accuracy of the $\delta^{36}S$ measurements do not allow deriving additional information on sulfur isotope systematics beyond that of $\delta^{33}S$. The results for $\delta^{36}S$ are reported in this study but not further discussed for this reason. The values for ${}^{33}\theta$ and ${}^{36}\theta$ used in this study were 0.515 and 1.90, respectively, if not otherwise indicated.

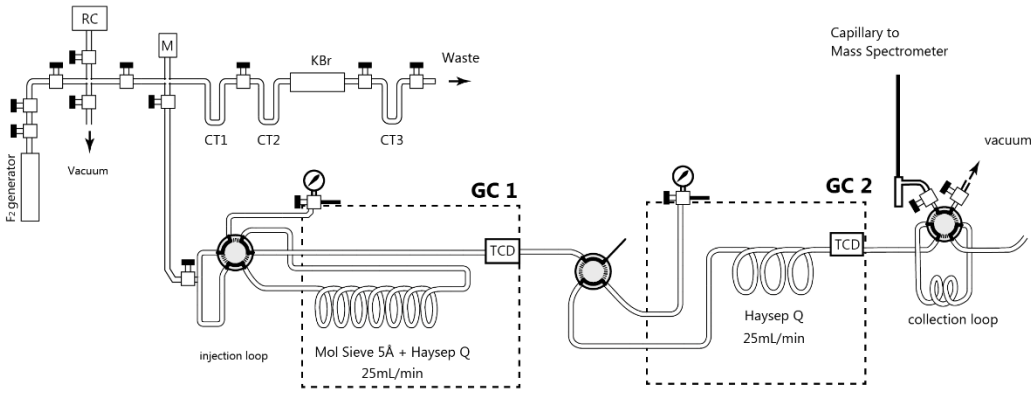

Figure 5 Outline of the Geophysical Laboratory laser fluorination dual-GC manifold for high precision multiple-sulfur isotope analysis. RC, reaction chamber; CT, cold traps; M, capacitance manometer; TCD, thermal conductivity detector. Figure reproduced and modified from Ono et al. (2006).

3 Results

The fluids sampled at Krafla, NE Iceland, are very dilute (14-235 ppm Cl) and represent both liquid water and vapor (Table 1). The concentration of SO_4 and ΣS^{-II} in the water phase of the well discharges was 5-525 ppm and 25-121 ppm, respectively, but S_2O_3 was also observed with concentrations in the range of 0.3 to 39 ppm (Table 2). Other sulfur compounds were not detected in the liquid phase. In the vapor phase H_2S was the only observed sulfur compound with concentrations between 44 and 1831 ppm. The sampling temperatures were between 138 and 437 °C.

In the water phase, the $\delta^{34}S$ values for ΣS^{-II} and SO_4 were -1.83 to -0.23 and +3.40 to +13.37 ‰, respectively. The $\delta^{34}S$ values for H_2S in the vapor phase were +0.05 to +1.28 ‰. The $\Delta^{33}S$ values were for ΣS^{-II} in the water phase were between -0.0187 and -0.0008 ‰, for SO_4 in the water phase between -0.0356 and -0.0044 ‰ and H_2S in the vapor phase between -0.0115 and -0.0001 ‰.

The distribution of $\delta^{34}S$ ratios in geothermal water and vapor, pyrite, sulfates, and altered and unaltered bulk rock in Iceland is shown in Figure 6. The data shown are those obtained in this study and previously reported by Sakai et al. (1980) and Torssander (1989). Unaltered basalt range in $\delta^{34}S$ from -2.0 to +0.4 ‰. Similar ratios were observed for ΣS^{-II} and H_2S in the geothermal water and vapor and pyrite for dilute geothermal systems or in the range of 0 to +2.6 ‰. On the other hand, pyrite for geothermal systems with seawater as the source fluid like at Reykjanes and Svartsengi have more positive ratios in the range of -1.5 to +7.9 ‰, suggesting seawater sulfate influence. Moreover, in the saline geothermal systems in Iceland, SO_4 in the water, rock and sulfate minerals have $\delta^{34}S$ values between +18.5 and +20.4 ‰, close to seawater value of 21.0 ‰ (Rees et al., 1978). In dilute geothermal systems, sulfate minerals are absent and the $\delta^{34}S$ range for aqueous SO_4 is between +3.40 and +13.37 ‰, much closer to the rock and sulfide than seawater sulfur isotope ratios.

Table 1 Chemical composition of two-phase well discharges at Krafla, NE Iceland.

Sample #	Well no	p^{sample}	*h*		Water phase (ppm)													Vapor phase (mmol/kg)					
		bar	kJ/kg	pH/C°	SiO_2	B	Na	K	Ca	Mg	Fe	Al	Cl	F	CO_2	SO_4	H_2S	CO_2	H_2S	H_2	N_2	CH_4	Ar
11-KRA-01	K-17	18.0	2399	8.80/23	641	1.37	129	20.5	0.27	0.009	0.027	1.49	17.9	1.82	83.9	5.4	102	102.37	24.13	22.85	1.61	0.18	0.03
11-KRA-02	K-16A	10.5	2660	7.35/24	653	2.00	194	31.7	0.85	0.004	0.028	1.06	138	1.76	230.1	10.8	72.0	481.70	38.96	35.12	1.02	0.33	0.03
11-KRA-03	K-37																						
11-KRA-04	K-32	9.5	1468	9.12/18	529	0.63	260	40.5	3.06	0.006	0.007	1.46	42.0	1.16	59.8	280	103	56.96	23.48	12.62	1.08	0.08	0.02
11-KRA-05	K-33	8.5	2769	8.42/19	775	2.92	161	28.7	0.75	0.004	0.025	0.43	97.6	1.89	162.3	7.3	120	75.84	45.59	27.04	1.14	0.03	0.02
11-KRA-06	K-20	10.5	2776	8.25/17	898	3.29	278	49.9	1.54	0.008	0.015	0.22	234	1.70	197.1	5.1	97.0	389.44	40.41	34.67	1.40	0.17	0.03
11-KRA-07	K-14																						
11-KRA-08	K-24	3.4	852	9.59/18	367	0.60	203	16.5	2.72	0.039	0.012	0.75	44.2	0.78	45.7	223	28.4	43.91	1.28	0.24	3.19	0.28	0.07
11-KRA-09	K-13A	8.0	1553	9.08/15	454	0.99	227	25.2	3.44	0.006	0.016	1.15	38.5	1.10	57.7	262	68.6	67.55	18.38	17.60	1.02	0.06	0.02
11-KRA-10	K-21	10.0	1058	8.90/21	513	0.74	173	23.0	1.33	0.002	< 0.010	1.33	135	0.93	54.0	54.7	42.0	67.65	11.74	6.54	2.94	0.85	0.06
11-KRA-11	K-05	3.4	998	9.22/16	351	0.59	203	17.8	3.05	0.024	0.012	0.85	41.4	0.98	51.1	218	27.6	20.31	5.16	1.07	2.92	0.20	0.06
11-KRA-12	K-27	11.5	1370	9.25/15	455	0.59	206	27.2	2.61	0.017	0.181	1.46	38.0	0.98	57.2	252	42.8	43.17	6.86	3.24	2.85	0.25	0.05
11-KRA-16	K-40	11.0	2774	6.49/9	520	2.83	85	15.1	2.11	0.049	0.024	1.45	20.7	1.61	925.8	19.9	32.8	473.31	30.38	8.70	26.71	0.12	0.35
11-KRA-17	K-34	17.5	2763	7.27/9	592	5.00	176	30.4	1.72	0.008	0.030	0.95	157.0	1.49	69.8	52.2	63.0	246.48	53.87	25.10	1.34	0.06	0.03
11-KRA-18		1																					
	IDDP-01	143	3200																				
	IDDP-01	143	3200																				

Table 2 Sulfur species concentration and sulfur isotope ratios in geothermal well discharges, Krafla NE Iceland. Concentrations are in ppm and isotope ratios in ‰.

Sample #	Well #	t^{sample}	$t^{reservoir\ a}$	*h*	Liquid phase										Vapor phase			
		°C	°C	kJ/kg	pH / °C	SO_4	ΣS^{-II}	S_2O_3	ΣS^{-II}			SO_4			H_2S	H_2S		
									$\delta^{34}S$	$\Delta^{33}S$	$\Delta^{36}S$	$\delta^{34}S$	$\Delta^{33}S$	$\Delta^{36}S$		$\delta^{34}S$	$\Delta^{33}S$	$\Delta^{36}S$
11-KRA-01	K-17	208	256[a]	2399	8.80 / 23	5.36	102	0.28	-1.25	-0.002	-0.064				821	0.50	-0.014	0.063
11-KRA-02	K-16A	181	240[a]	2660	7.35 / 24	10.8	72.0	4.82	-0.67	-0.001	-0.001				1326	1.26	-0.004	0.029
11-KRA-03	K-37															1.28	-0.012	-0.022
11-KRA-04	K-32	177	234[a]	1468	9.12 / 18	280	103	0.27	-1.11	-0.016	-0.150	4.66	-0.008	0.089	799	1.04	0.000	0.037
11-KRA-05	K-33	173	230[a]	2769	8.42 / 19	7.26	120	1.44	-1.06	-0.009	0.046				1551	0.33	-0.009	0.015
11-KRA-06	K-20	181	240[a]	2776	8.25 / 17	5.10	97.0	0.42	-1.53	-0.008	-0.136				1375	0.05	-0.016	0.109
11-KRA-07	K-14															0.84	-0.011	-0.028
11-KRA-08	K-24	138	175[a]	852	9.59 / 18	223	28.4	1.89	-1.19	-0.010	0.059	4.29	-0.018	-0.026	44	1.20	-0.009	-0.019
11-KRA-09	K-13A	171	220[a]	1553	9.08 / 15	262	68.6	3.41	-1.73	-0.009	0.054	4.38	-0.016	0.026	625	0.55	-0.001	0.068
11-KRA-10	K-21	179	234[a]	1058	8.90 / 21	54.7	42.0	1.28	-1.70	-0.012	0.144	6.11	-0.029	0.129	400	0.78	-0.003	0.041
11-KRA-11	K-05	138	201[a]	998	9.22 / 16	218	27.6	9.26	-1.83	-0.010	0.104	3.40	-0.004	0.051	176	0.78	-0.004	0.073
11-KRA-12	K-27	185	223[a]	1370	9.25 / 15	252	42.8	28.2	-0.97	-0.019	0.000	3.82	-0.015	0.063	233	1.11	-0.005	0.017
11-KRA-16	K-40	183	192[a]	2774	6.49 / 9	19.9	32.8	6.43	-0.23	-0.001	0.034	13.37	-0.036	0.167	1034	0.64	-0.010	-0.044
11-KRA-17	K-34	207	235[a]	2763	7.27 / 9	52.2	63.0	39.1	-0.51	-0.015	-0.043	9.78	-0.025	-0.020	1833	1.06	-0.014	0.049
	IDDP-1	437	437[a]	3200											668	1.13	-0.014	-0.099
	IDDP-1	437	437[a]	3200											617	0.52	-0.001	0.020

[a] Reservoir temperature calculated using the quartz geothermometer (Gunnarsson and Arnórsson, 2000) The values reported are the average calculated values using the three models for reconstructed reservoir fluid composition (see text). In the case of dry steam discharge the sampling temperatures are just reported.

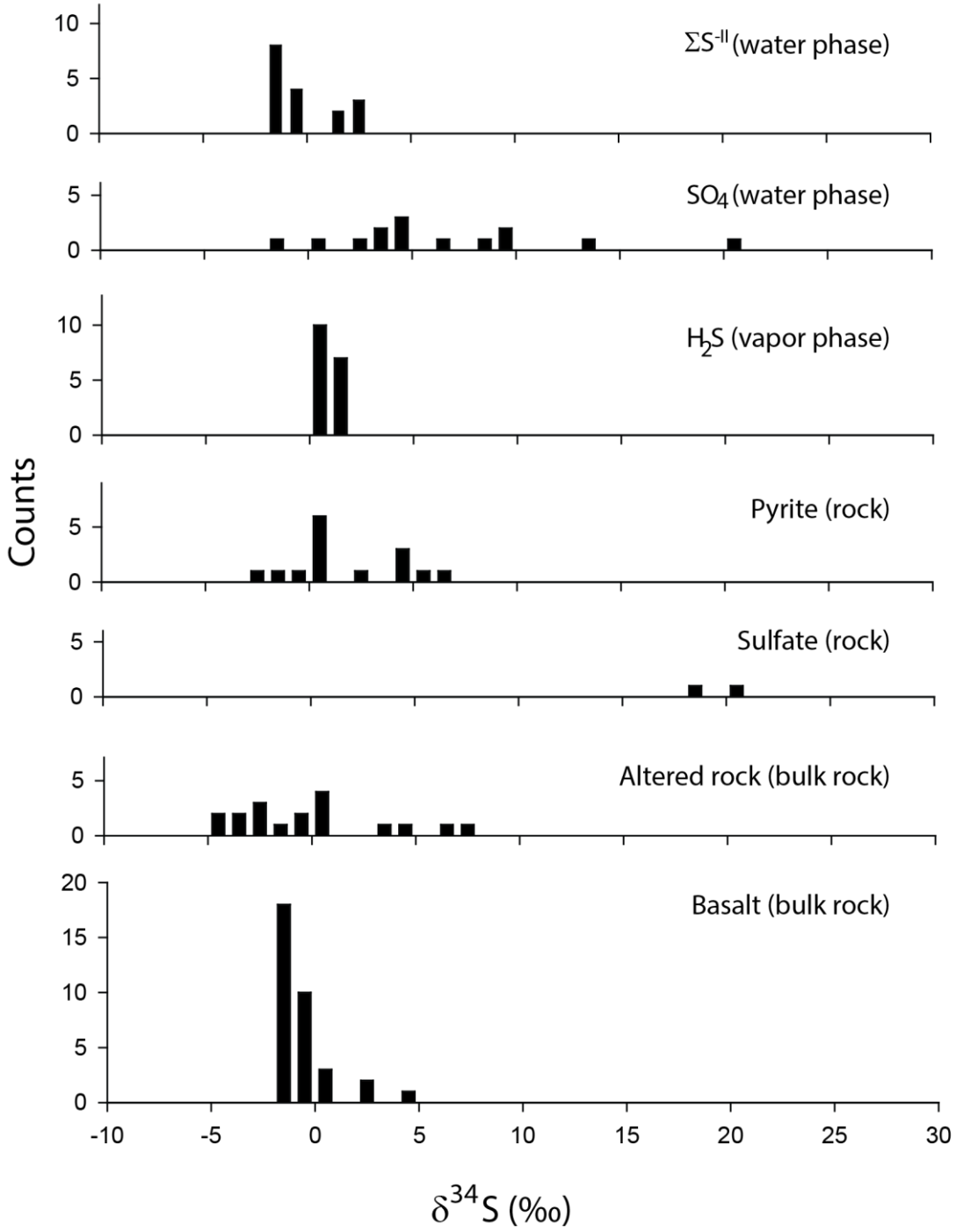

Figure 6 Distribution of $\delta^{34}S$ in geothermal water, vapor, geothermal altered rocks and fresh basalts in Iceland. All data available at current time are shown. The results presented are those obtained in this study (Table 1) as well as those previously reported by Sakai et al. (1980) and Torssander (1989).

4 Discussion

4.1 Reservoir geothermal fluid composition and sulfur speciation

Assessment of sulfur chemistry and isotope systematics in the reservoirs of volcanic geothermal systems relies on the reconstruction of reservoir fluid compositions from samples and analysis of the liquid and vapor discharged at the surface from wells drilled into the reservoir. The reservoirs may be sub-boiling with a liquid only phase; consist of two phases, liquid and vapor; or be a single vapor phase. For liquid only sub-boiling reservoirs, depressurisation boiling occurs within the well. In this case it is reasonable to assume the system to be isolated, i.e. the enthalpy and mass is conserved upon fluid ascent to the surface. Wells discharging such reservoirs have surface enthalpies typically < 1200 kJ/kg for reservoir temperatures < 300°C. In the case of two-phase liquid and vapor only systems intensive boiling occurs within the reservoir. Such boiling may either be caused by pressure drop within the reservoir or by addition of heat, for example from a magma body or both. This leads to excess discharge enthalpies exceeding the initial fluid enthalpy, typically > 1500 kJ/kg. Depressurisation boiling leads to temperature decrease of the fluid along the two-phase curve of water whereas conductive heat addition boiling leads to a constant temperature until pure vapor is formed (Henley and Hughes, 2000). Consideration of the physical properties of liquid water and vapor, fluid flow and chemical variability of well discharges as a function of discharge enthalpy suggest that depressurisation boiling within the reservoir may lead to phase segregation (e.g. Arnórsson et al., 2007; Scott et al., 2014). In this case, the liquid phase is retained on mineral grain surfaces and the lower density vapor preferentially flows towards the well. The strong decrease in the relative permeability of liquid at intermediate vapor saturations and high capillary pressures contribute to causing liquid to adhere to mineral grain surfaces and remain in the reservoir (Sorey et al., 1980, Horne et al., 2000, Pritchett, 2005; Li and Horne, 2007). The two-processes causing excess discharge enthalpy and reservoir vapor, conductive heat addition and vapor-liquid phase segregation, results in very different concentrations patterns of non-volatiles in the fluid discharge with increasing discharge enthalpy. Conductive heat addition leads to increased concentration of non-volatiles in the liquid phase, whereas the concentration in the total discharge remains constant with increasing enthalpy. On the other hand, vapor-liquid phase segregation leads to constant concentration of a non-volatile in the liquid phase as a function of enthalpy whereas the concentration in the total discharge decreases.

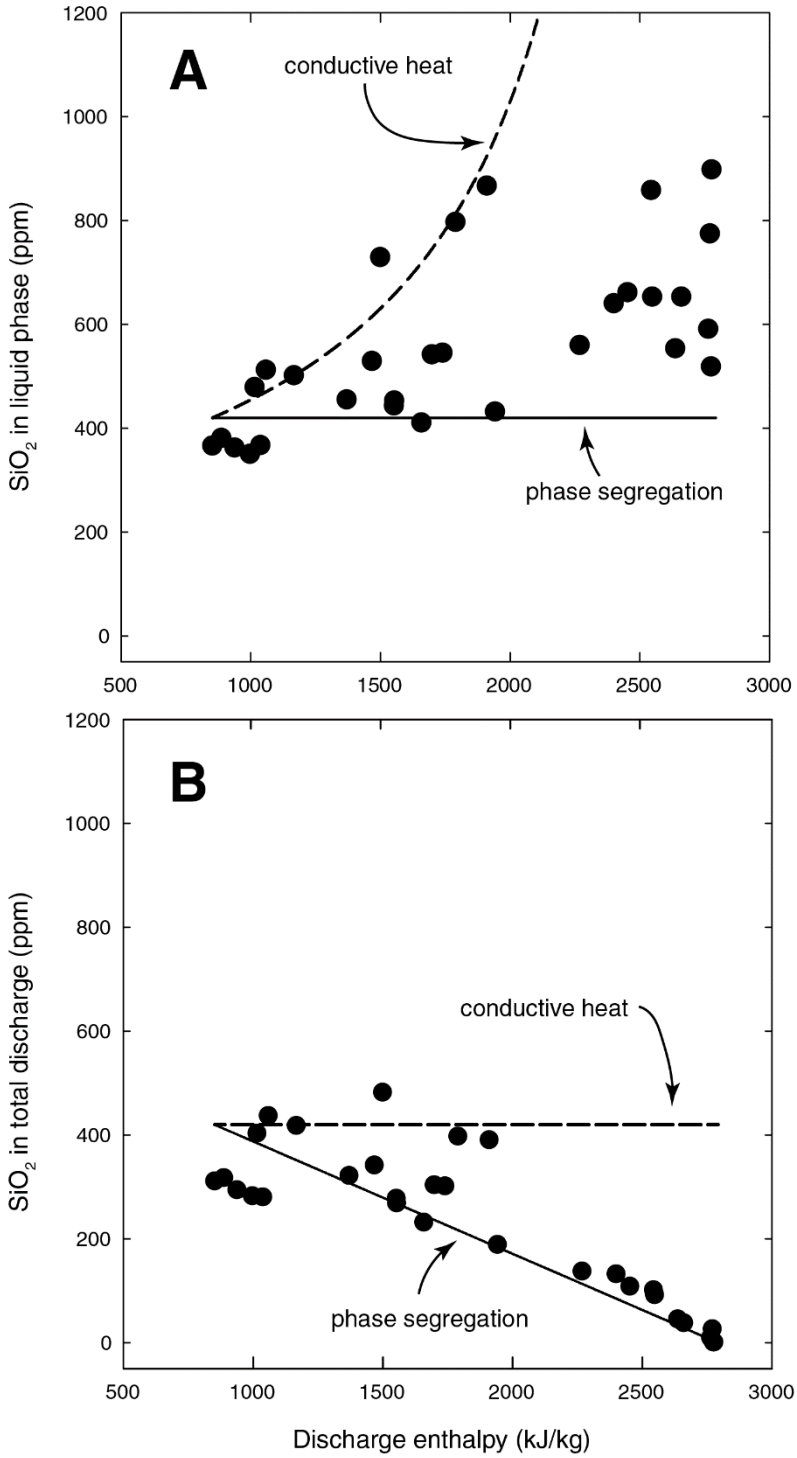

Figure 7 The concentration of SiO_2 in the liquid phase and total two-phase discharge as a function of discharge enthalpy. The effects of conductive heat addition and phase segregation were calculated at constant temperature of 200°C and for fluids having initial SiO_2 concentration of 420 ppm. The calculations were carried out with the aid of the WATCH program. As observed, two processes are likely to be the cause of excess discharge well enthalpy, or too high vapor to liquid ratio relative to the reservoir temperature and assuming liquid only reservoir. Firstly, the excess vapor may be the result of conductive heat in the reservoir, for example from a magma body, causing reservoir vapor fraction. Alternatively, drilling may have resulted in pressure drawdown in the reservoir resulting in reservoir boiling and vapor and liquid separation. The data shown in the plot are those obtained in this study together with literature data (Gudmundson and Arnórsson, 2005; Giroud, 2008).

Many of the well discharges at Krafla show excess enthalpy character, the cause being either or both phase segregation and conductive heat addition (Fig. 7). In this study, the reservoir fluid compositions were calculated from two-phase well discharges assuming that the excess enthalpy of the well discharges was the consequence of either phase segregation or heat addition. In addition, the reservoir fluid composition was calculated assuming no vapor in the reservoir. The three models applied are referred to as isolated system boiling model (no vapor in the reservoir), conductive heat model (excess enthalpy caused by heat addition) and phase segregation model (excess enthalpy caused by depressurisation boiling followed by phase segregation). The calculations were carried out using the WATCH program (Bjarnason, 2010) and are based on formulation derived and given by Arnórsson et al. (2007). Three parameters are needed in order to calculate the reservoir fluid composition from the wellhead data, temperature and enthalpy of the well discharge and the reservoir and the temperature or pressure where phase segregation occurred. For the present study the reservoir temperature was based on the quartz geothermometer (Gunnarsson and Arnórsson, 2000). Selection of the phase segregation temperature or pressure is less straightforward, as phase segregation likely occurs over a temperature or pressure interval rather than at a single point. Following Arnórsson et al. (2007) the segregation temperature was assumed to be approximately halfway between the initial reservoir fluid temperature and the wellhead temperature.

It is generally accepted that the concentrations of major elements in geothermal fluids, except that incompatible elements like Cl are controlled by near equilibrium with secondary minerals observed in the geothermal systems (e.g. Giggenbach, 1980, 1981; Arnórsson et al., 1983). On the other hand, redox equilibria may not be attained between aqueous species and gases in the system H-O-S-C-N, even at temperatures as high as 300°C (Stefánsson and Arnórsson, 2002). In addition, isotope equilibrium among H_2S and SO_4 in geothermal fluids have been observed to be in isotope disequilibrium (Ohmoto and Lasaga, 1982). In order to assess chemical equilibrium among the common sulfide minerals and sulfur species at Krafla, the following reactions were considered,

$$\text{pyrite} + H_2S(aq) = \text{pyrrhotite} + H_2(aq) \quad (4)$$

and oxidation of aqueous sulfide to form thiosulfate and sulfate according to the reactions,

$$H_2S(aq)+1.5H_2O = S_2O_3^{2-}(aq) + H^+ + 2H_2(aq) \quad (5)$$

$$H_2S(aq)+4H_2O = SO_4^{2-}(aq) + 2H^+ + 4H_2(aq) \quad (6)$$

Pyrite and pyrrhotite have both been observed to occur within the Krafla geothermal system (Steinthórsson and Sveinbjörnsdóttir, 1981) and ΣS^{-II}, SO_4 and S_2O_3 in water and H_2S in vapor are the only detected sulfur components in the fluids (Kaasalainen and Stefánsson, 2011b).

The aqueous species activities were calculated with the aid of the WATCH program (Bjarnason et al. 2010) from the reservoir composition calculated using the three approaches discussed above. Additional data on fluid discharges reported by Gudmundsson and Arnórsson (2005) and Giroud (2008) were also included on the plots together with the data reported in Table 1. The equilibrium constants for the respective reactions were calculated using the Supcrt92 program (Johnson et al. 1992) and the slop07.dat database (http://geopig.asu.edu/sites/default/files/slop07.dat). The equilibrium conditions were calculated at 200 and 300°C at water vapor saturation pressure (P_{sat}) and 400 and 500°C at 500 bar.

The results of chemical equilibrium among sulfur bearing minerals and aqueous species largely relies on the approach for calculating the reservoir composition (Fig. 8). The reservoir temperatures, calculated using the quartz geothermometer, were in the range of 192-330°C as well as the IDDP-1 well with a temperature of 437°C. This is somewhat lower than the predicated equilibrium temperatures for the various sulfur bearing minerals and redox. The causes for these discrepancies may be many. Firstly, problems related to sampling and chemical analysis may contribute, however, this source of error is considered unlikely and sampling and analytical techniques used here are considered reliable (e.g. Arnórsson et al., 2006; Kaasalainen and Stefánsson, 2011a, 2011b). Secondly, the thermodynamic data, both used for the aqueous speciation and to predict the reaction equilibrium constants, may be uncertain. For example, Pokrovski and Dubrovinsky (2011) suggested that S^{3-} may be a key fluid species in hydrothermal fluids at > 300°C, this species is not included here. Thirdly, the aqueous speciation of sulfur compounds at reservoir conditions may not represent the sampling conditions and reactions may occur within the well upon fluid ascent to surface. However, it should be kept in mind that the temperature change from reservoir to surface sampling is usually < 100°C. Based on these facts and following Stefánsson and Arnórsson (2002) it is difficult to assess if overall equilibrium exists among sulfur species and sulfur-bearing minerals under hydrothermal conditions in dilute fluids at < 300°C like those observed at Krafla.

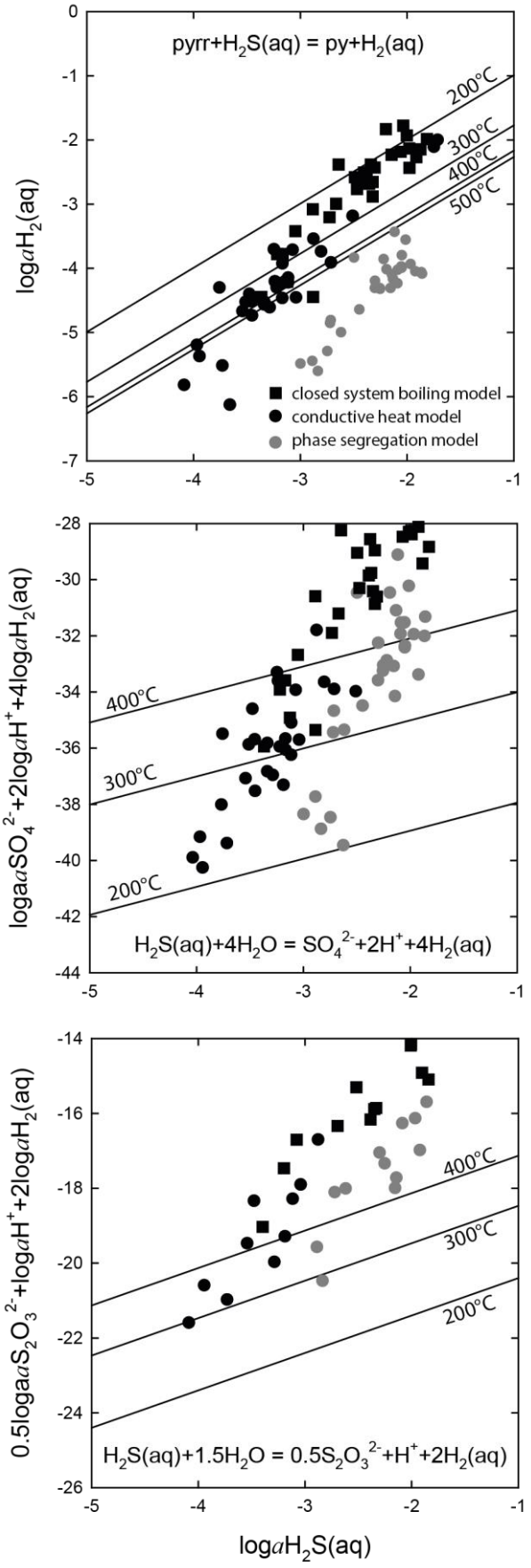

Figure 8 Mineral buffer equilibria among H_2S and SO_4 bearing minerals. Shown are the calculated activity products for given reactions and these compared with the calculated equilibrium concentrations at 200 and 300°C and water vapor saturation pressure and 400 and 500°C at 500 bar. The results of the three models used for calculation of the reservoir fluid composition based on fluid well discharge at surface are shown.

4.2 Sulfur isotope systematics upon boiling and water rock interaction and geothermal reservoir sulfur isotope ratios

In order to reconstruct the sulfur isotope ratios in the geothermal reservoir from data on well water and vapor samples collected from the well discharge, the boiling models discussed previously were extended to include multiple sulfur isotope fractionations upon vapor-liquid interaction and associated aqueous species distribution changes. The calculations essentially involved two steps. First, calculating water and vapor distribution upon boiling and the associated aqueous and vapor speciation and second, sulfur isotope distribution among the aqueous and vapor species in the water and vapor phases. The aqueous species included in the calculations upon boiling were $H_2S(g)$, $H_2S(aq)$ and HS^-. Aqueous SO_4 was not included as it does not partition between the water and vapor phase upon boiling and $SO_4^{2-}(aq)$ predominates the aqueous species concentrations under all conditions. It follows that measured SO_4 isotope ratios of surface discharge reflect those of the reservoir.

For the reconstruction of the reservoir fluid isotope ratios the system was assumed to be isotopically closed upon boiling, i.e. a mass balance equation can be defined accordingly,

$$\delta^x S^{total} = X_{H_2S(g)}\delta^x S_{H_2S(g)} + X_{H_2S(aq)}\delta^x S_{H_2S(aq)} + X_{HS^-}\delta^x S_{HS^-} \quad (7)$$

where X_i are the appropriated mole fractions of $H_2S(g)$, $H_2S(aq)$ and HS^- and x stands for sulfur 33, 34 or 36. The fractionation factor α between two aqueous and/or gas species i and j is defined by,

$$^x\alpha = 1000 + \delta^x S_i / 1000 + \delta^x S_j \quad (8)$$

Combining the fractionation factors relative to $H_2S(aq)$ (Eq. 8) and the sulfur isotope mass balance equation (Eq. 7) we obtain,

$$\begin{aligned}\delta^x S^{total} &= X_{H_2S(aq)}\delta^x S_{H_2S(aq)} \\ &+ X_{H_2S(g)}\left(\left(^x\alpha_{H_2S(g)-H_2S(aq)}\left(1000 + \delta^x S_{H_2S(aq)}\right)\right) - 1000\right) \\ &+ X_{HS^-}\left(\left(^x\alpha_{HS^- - H_2S(aq)}\left(1000 + \delta^x S_{H_2S(aq)}\right)\right) - 1000\right)\end{aligned} \quad (9)$$

Knowing the isotope fractionation factors, $\delta^x S^{total}$ and the mole fraction of the appropriated aqueous and vapor species, the isotope ratios for $H_2S(g)$, $H_2S(aq)$ and $HS^-(aq)$ were calculated using non-linear regression. The values for the fractionation factors are given in Table 3 and are based on values reported by Ohmoto and Rye (1979), Otake et al. (2008) and Czarnacki and Halas (2012). Smoothed fractionation factors were obtained in this study by fitting the reported values to a function of $10^3 \ln\alpha = A+B/T+C/T^2$ using non-linear least squares regression.

The effects of boiling upon multiple sulfur isotope fractionation is demonstrated in Figures 9 and 10. Depressurisation boiling along the water vapor saturation curve results in partitioning of volatile species like H_2S and CO_2 into the vapor phase. This results in a pH increase of the water phase and changes in aqueous speciation including ionisation of $H_2S(aq)$ to form HS^-. The $H_2S(g)$ and $H_2S(aq)$ species are isotopically similar, yet $H_2S(aq)$ becomes progressively heavier relative to $H_2S(g)$ upon progressive boiling. Sulfur isotope fractionation

between H_2S(aq) and HS^-(aq) is, however, significant or approximately -4 to -2.5 ‰ at 100-300°C. The combined changes in aqueous speciation and vapor formation upon boiling results in the water phase becoming isotopically lighter with progressive boiling whereas the vapor phase becomes isotopically heavier.

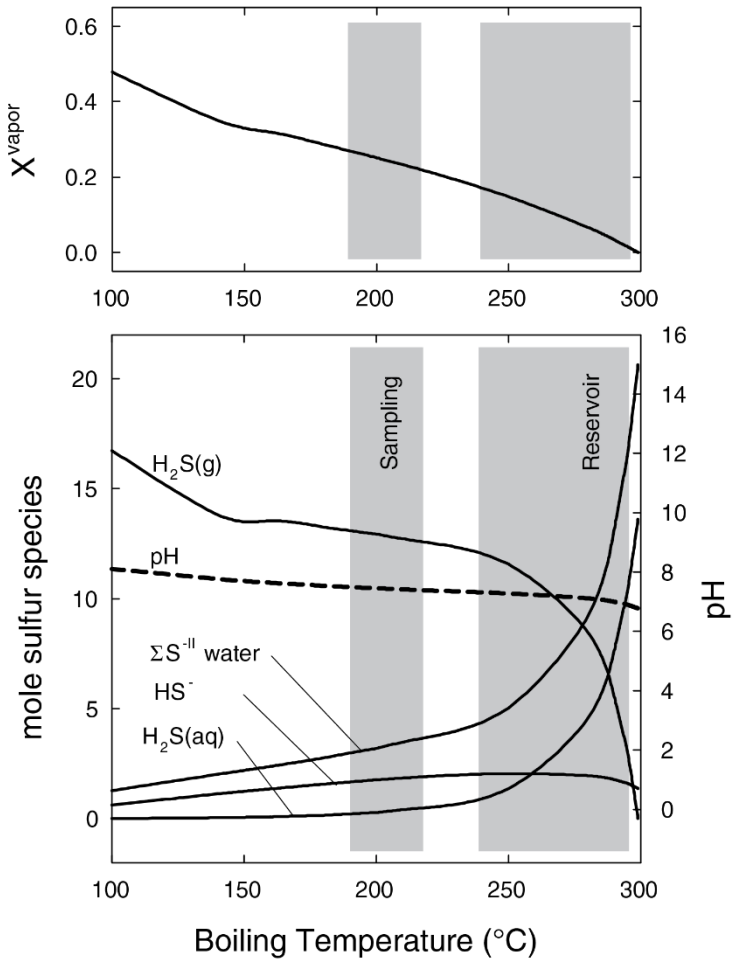

Figure 9 The effects of closed system boiling on aqueous speciation of sulfide sulfur. Upon depressurisation boiling H_2S(aq) partitions into the vapor phase resulting in increased H_2S(g) mole fraction and decreased dissolved sulfide in the water phase, i.e. $\Sigma S^{-II} = H_2S(aq)+HS^-$. This together with loss of CO_2 into the vapor phase leads to increased pH of the boiled water resulting in the ionisation of H_2S(aq) to HS^-. Also shown (gray shaded areas) are the range of reservoir and sampling temperatures at Krafla.

Fluid-rock interaction is considered among the major effects on sulfur chemistry and isotope systematics in geothermal systems. In order to study possible variations in sulfur concentrations and sulfur isotope systematics a geochemical model was developed that takes into account possible sources and reactions of sulfur and sulfur isotopes upon progressive dissolution of primary rocks and formation of secondary minerals including sulfides. In the model meteoric water was allowed to react with basalt in steps and the saturated secondary minerals allowed to precipitate. The composition of the basaltic glass, the starting solution and the secondary minerals incorporated in the calculations were taken from Kaasalainen and Stefánsson (2012). The basaltic glass was taken to contain 350 ppm S (Gunnlaugsson, 1977). This part of the modelling is a conventional reaction path model and was conducted with the aid of the PHREEQC program (Parkhurst and Appelo, 1999). From the reaction path

calculation the mole distribution of dissolved sulfide and sulfate species was obtained as well as the mass of secondary minerals formed as a function of the reaction progress (ξ). The sulfur species observed to be significant were $H_2S(aq)$, $HS^-(aq)$ and SO_4^{2-} and the only secondary sulfur bearing mineral predicated to form was pyrite. The mass fraction of the sulfur species and sulfur bearing minerals formed was subsequently combined with the multiple sulfur isotope fractionation factors (Table 3) to calculate sulfur isotope distribution in a similar manner as previously described according to

$$\delta^{x}S^{\text{total}} = X_{H_2S(aq)}\delta^{x}S_{H_2S(aq)} + X_{HS^-}\left(\left({}^{x}\alpha_{HS^- - H_2S(aq)}\left(1000 + \delta^{x}S_{H_2S(aq)}\right)\right) - 1000\right) + X_{\text{pyrite}}\left(\left({}^{x}\alpha_{\text{pyrite} - H_2S(aq)}\left(1000 + \delta^{x}S_{H_2S(aq)}\right)\right) - 1000\right) \quad (10)$$

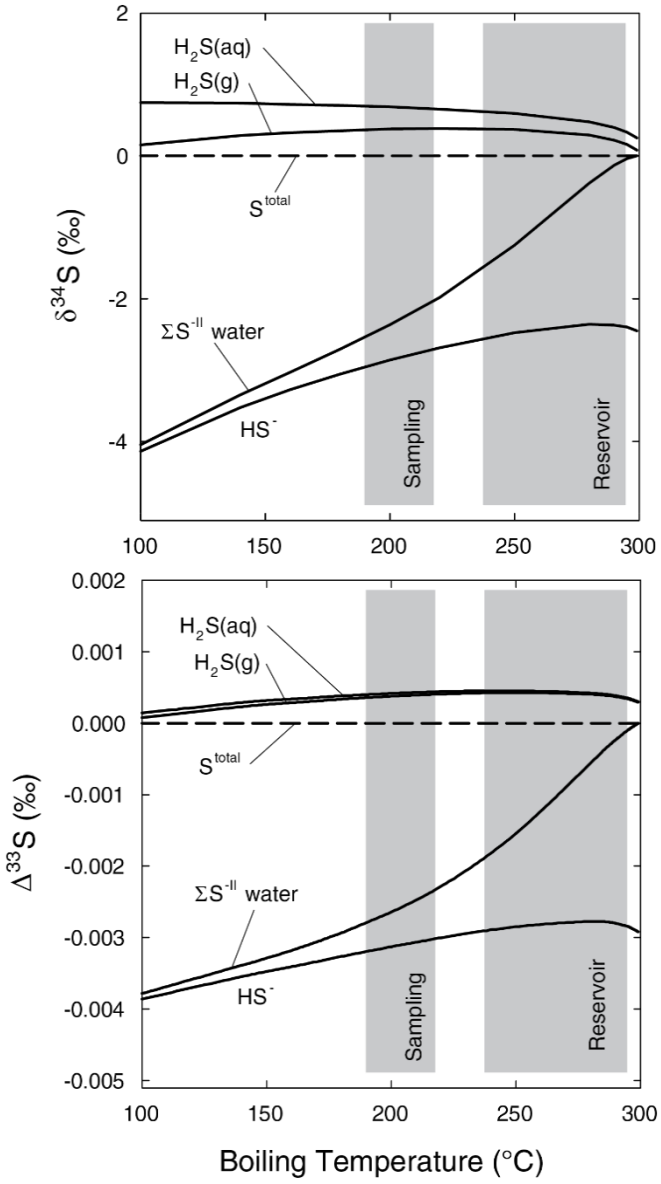

Figure 10 The effects of closed system boiling on sulfur isotope ratios ($\delta^{34}S$ and $\Delta^{33}S$) of $H_2S(g)$, $H_2S(aq)$, HS^- and total dissolved sulfide in the water phase, i.e. ΣS^{-II} = $H_2S(aq)+HS^-$. Upon boiling the $H_2S(aq)$ becomes isotopically heavier relative to $H_2S(g)$ as one would expect. However, associated with the boiling and acid loss to the vapor phase, the solution pH increases and $H_2S(aq)$ ionizes to HS^- causing large sulfur isotope fractionations and leading to lighter sulfur isotope ratios of the water phase.

The results of the mole fraction distribution of aqueous $H_2S(aq)$, $HS^-(aq)$ and pyrite and sulfur isotope ratios under geothermal conditions as a function of reaction progress (ξ) is shown in Figure 11. The total sulfur isotope ratio of the system ($\delta^x S^{total}$) was taken to be unity. The results demonstrate that upon progressive fluid-rock interaction sulfur is leached out of the primary rocks in the form of sulfide under the reduced conditions observed under geothermal conditions. This eventually leads to pyrite formation and sulfur isotope fractionation, resulting in the fluids becoming progressively lighter relative to pyrite upon the reaction progress.

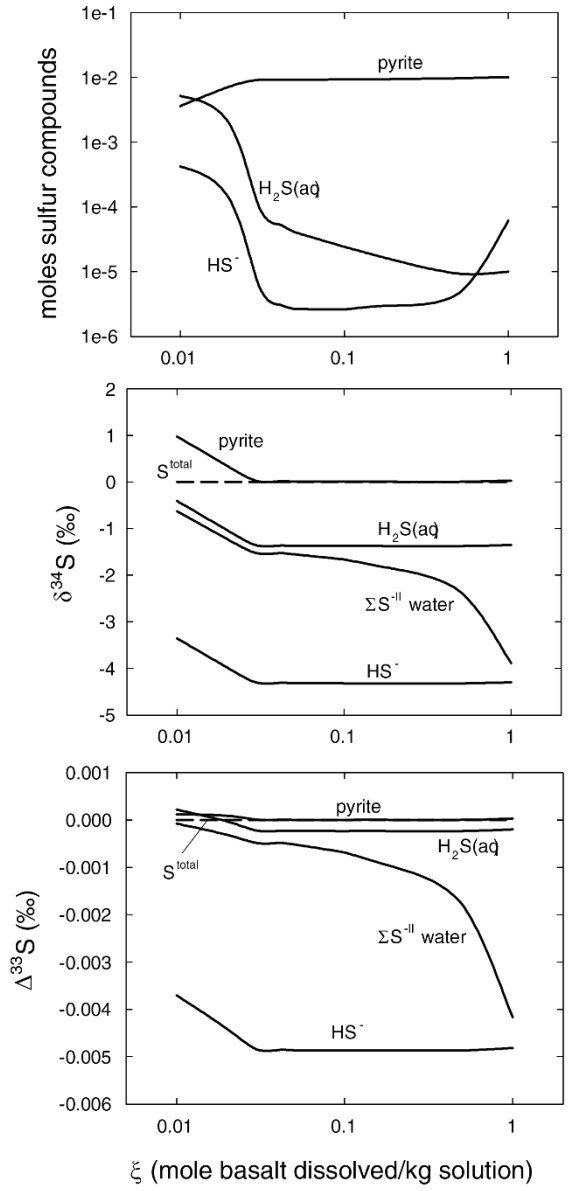

Figure 11 The effect of progressive fluid-rock interaction on sulfur compound mole fractions and sulfur isotope ratios ($\delta^{34}S$ and $\Delta^{33}S$) of $H_2S(aq)$, HS^- and total dissolved sulfide in the water phase, i.e. $\Sigma S^{-II} = H_2S(aq)+HS^-$, and pyrite. The $\delta^{34}S$ and $\Delta^{33}S$ isotope ratios of the system were assumed to be zero. Upon progressive rock (basalt) dissolution (ξ) sulfide sulfur is leached from the rock eventually leading to pyrite formation and the pH of the water is found to increase. As a result, total dissolved sulfide in the water phase becomes isotopically lighter relative to pyrite.

The effects of multiple sulfur isotope systematics upon boiling and progressive water rock interaction in geothermal systems like at Krafla are shown in Figure 12. Depressurisation boiling upon fluid ascent and progressive fluid-rock interaction and pyrite formation results in the liquid phase becoming progressively isotopically lighter relative to the total system, both with respect to $\delta^{34}S$ and $\Delta^{33}S$. In contrast, the $H_2S(g)$ in the vapor phase and pyrite formed become isotopically heavier upon boiling and fluid-rock interaction, respectively. These results are in good agreement with the measured sulfur isotope ratios for the vapor and water phases of the two-phase well discharges, with $\delta^{34}S$ ratios of the vapor phase being heavier relative to $\delta^{34}S$ ratios of the water phase that always display negative values. Similar observations are made for $\Delta^{33}S$ ratios, with the vapor phase being heavier relative to the water phase.

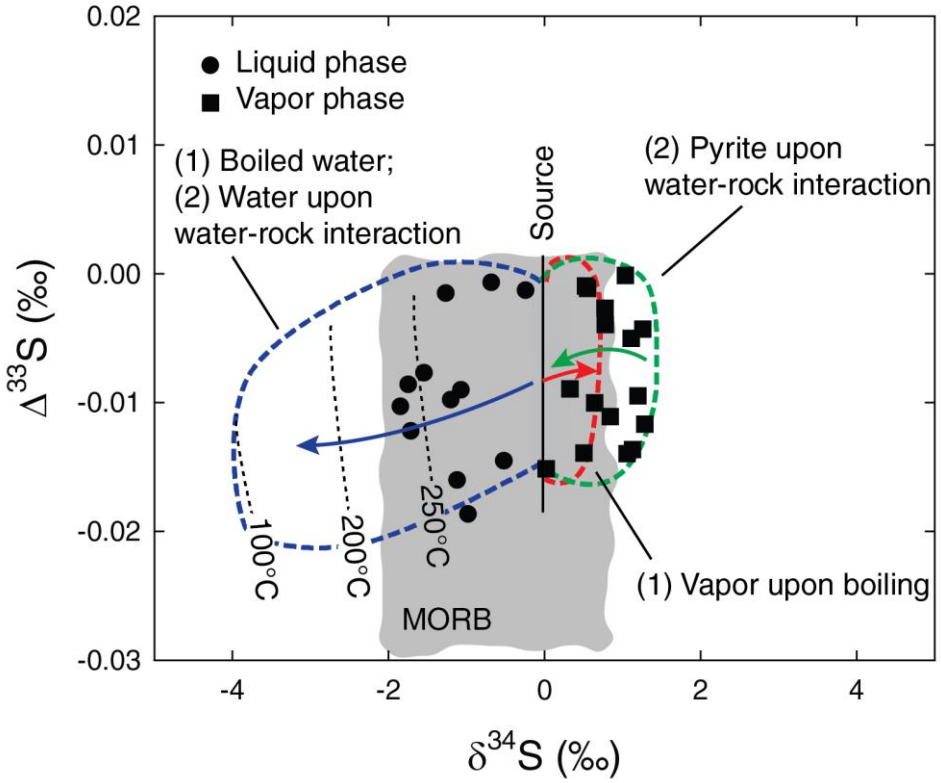

Figure 12 Summary of the relationship between $\Delta^{33}S$ and $\delta^{34}S$ for sulfide in the water phase, vapor phase and pyrite upon depressurisation boiling (as in shown in Figure 10, (1) on plot) and fluid-rock interaction (as shown in Figure 11, (2) on plot). Shown are the results of the various models for initial fluids of $\delta^{34}S$ equal to unity and $\Delta^{33}S$ in the range -0.015 to 0.000 ‰. Upon depressurisation boiling and progressive fluid-rock interaction the water phase becomes isotopically lighter relative to the source fluid with respect to $\delta^{34}S$ and $\Delta^{33}S$ ratios. In contrast, the vapor phase and pyrite becomes isotopically heavier with respect to $\delta^{34}S$ and $\Delta^{33}S$ ratios. This is indeed what is observed for two-phase well discharge fluids that have undergone boiling upon ascent to surface. Also shown are the range of $\Delta^{33}S$ and $\delta^{34}S$ observed for Icelandic basalts and MORB (Sakai et al., 1980; Torssander, 1989; Labidi et al., 2012; Ono et al., 2012).

The conclusions drawn here are that the source of sulfide sulfur in the Krafla geothermal fluids is of mid ocean ridge basalt (MORB) originating with $\delta^{34}S$ ratios close to unity or in the range -2 to +0.4 ‰ (Sakai et al., 1980; Torssander, 1989) and $\Delta^{33}S$ between -0.03 and 0.00 ‰ (Ono et al., 2012, Labidi et al., 2012). The $\delta^{34}S$ and $\Delta^{33}S$ variations of sulfide in the water and vapor phase are then caused by secondary processes, mainly boiling and progressive fluid-rock interaction, leading to an isotopically heavier vapor phase and isotopically lighter water phase. Distinguishing between the effects of boiling and fluid-rock interaction and sulfide mineralisation on the multiple isotope systematics is, however, difficult.

Based on these findings the reservoir multiple sulfur isotope ratios were calculated based on the three boiling models described previously. The results are listed in Table 4. As observed, somewhat variable results are obtained based on the model used, i.e. if the excess discharge enthalpy is assumed to be caused by conductive heat addition or depressurisation boiling and phase segregation. However, they all show close to the $\delta^{34}S$ ratios observed for unaltered Icelandic basalts pointing towards the source of sulfide sulfur in these systems (Fig. 13). On the other hand, $\delta^{34}S$ values for SO_4 are much higher or in the range of +3.40 to +13.37 ‰.

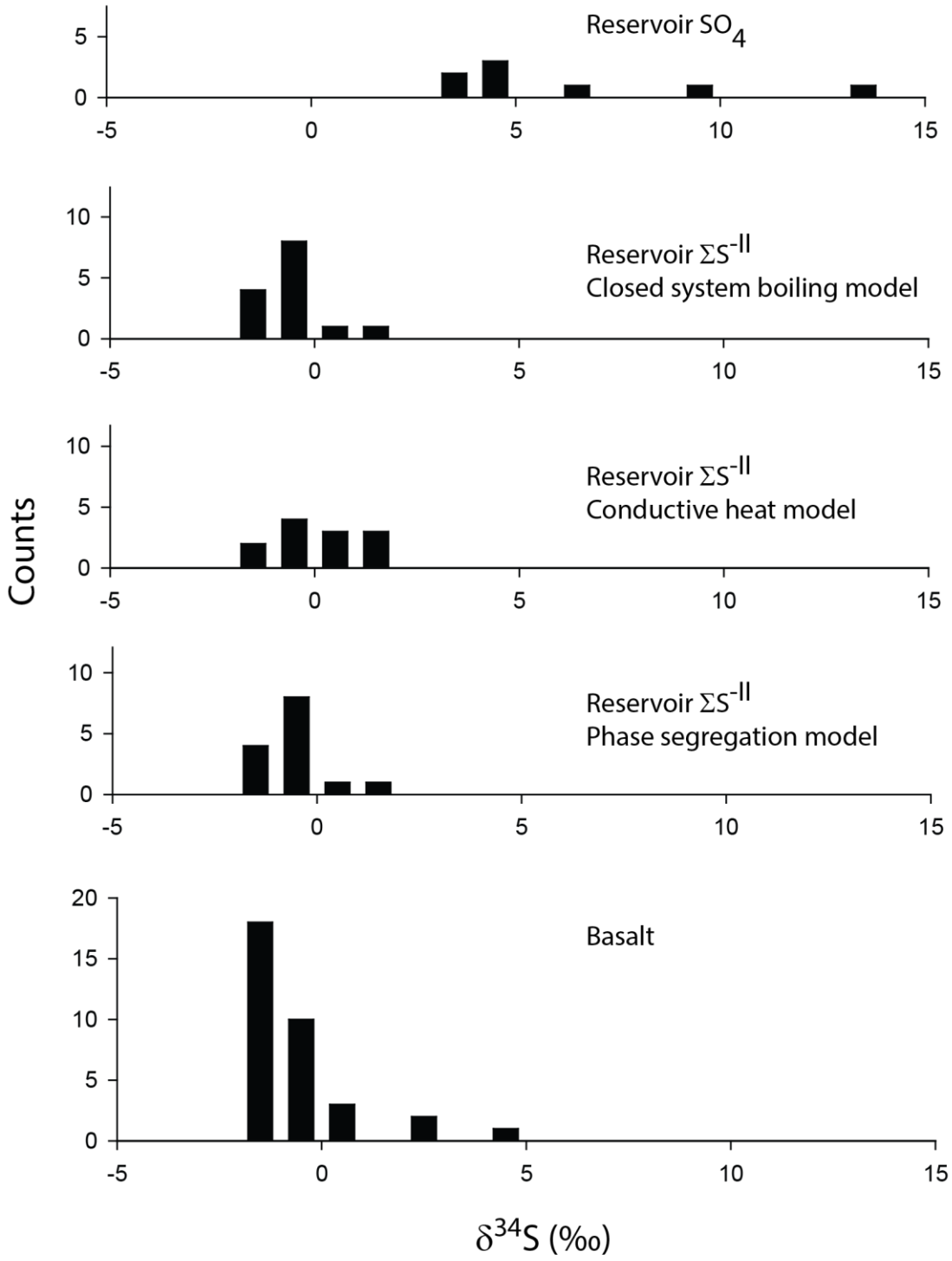

Figure 13 The calculated $\delta^{34}S$ ratios of reservoir fluids applying the three models for reconsruction of reservoir fluids from data on well fluid discharge (see text). As observed, the reservoir sulfide ratios of the reservoir fluids are very similar to those observed in basaltic rocks in Iceland (Sakai et al., 1980;Torssander, 1989) suggesting the same source of sulfide sulfur as in basalt either by magma degassing or basalt dissolution. Reservoir fluid sulfate ratios are heavier compared to sulfide ratios.

Table 3 Temperature functions to calculate smoothed fractionation factors of sulfur 33, 34 and 36 isotope ratios. The functions are based on values reported by Ohmoto and Rye (1979), Otake et al. (2008) and Czarnacki and Halas (2012).

	$10^3 \ln\alpha = A+B/T+C/T^2$								
	$^{33}\alpha$			$^{34}\alpha$			$^{36}\alpha$		
	A	B	C	A	B	C	A	B	C
$\alpha_{H_2S(g)-H_2S(aq)} = \frac{1000+\delta^x S_{H_2S(g)}}{1000+\delta^x S_{H_2S(aq)}}$	0.0301147	44.495329	-63232.52	0.05847522	86.398698	-122781.59	0.1111029	164.15753	-233285.02
$\alpha_{HS^- - H_2S(aq)} = \frac{1000+\delta^x S_{HS^-}}{1000+\delta^x S_{H_2S(aq)}}$	0.5060551	-1008.9084	-44883.045	0.97597038	-1947.3864	-90069.458	1.8534845	-3682.8757	-165168.62
$\alpha_{SO_4^{2-}-H_2S(aq)} = \frac{1000+\delta^x S_{SO_4^{2-}}}{1000+\delta^x S_{H_2S(aq)}}$	-3.7999529	5268.1093	1753303.1	-7.34135139	10167.868	3421169.4	-13.784628	19056.652	6553556.5
$\alpha_{pyrite-H_2S(aq)} = \frac{1000+\delta^x S_{pyrite}}{1000+\delta^x S_{H_2S(aq)}}$	0	0	206000	0	0	400000	0	0	760000

Table 4 Multiple sulfur isotope ratios in reservoir fluids calculated from the isotope composition of the discharge fluids and the appropriated model to reconstruct the reservoir fluids.

Sample #	Well #	Reservoir vapor phase			Total S^{-II} reservoir (vapor+liquid)								
		SO_4			*Closed boiling model*			*Conductive heat model*			*Phase segregation model*		
		$\delta^{34}S$	$\Delta^{33}S$	$\Delta^{36}S$	$\delta^{34}S$	$\Delta^{33}S$	$\Delta^{36}S$	$\delta^{34}S$	$\Delta^{33}S$	$\Delta^{36}S$	$\delta^{34}S$	$\Delta^{33}S$	$\Delta^{36}S$
11-KRA-01	K-17				-0.99	-0.003	-0.045	0.14	-0.011	0.037	-0.74	-0.005	-0.027
11-KRA-02	K-16A				-0.30	-0.001	0.004	1.15	-0.004	0.027	-0.17	-0.002	0.006
11-KRA-03													
11-KRA-04	K-32	4.66	-0.008	6.539	-0.78	-0.014	-0.121	-0.35	-0.010	-0.084	-0.58	-0.012	-0.104
11-KRA-05	K-33				-0.72	-0.009	0.039				-0.71	-0.009	0.038
11-KRA-06	K-20				-1.10	-0.010	-0.070				-1.23	-0.009	-0.089
11-KRA-07					0.84	-0.011	-0.028						
11-KRA-08	K-24	4.29	-0.018	5.922				-0.82	-0.010	0.047	-0.59	-0.010	0.040
11-KRA-09	K-13A	4.38	-0.016	6.090	-1.42	-0.008	0.056	-0.80	-0.006	0.060	-1.23	-0.007	0.057
11-KRA-10	K-21	6.11	-0.029	8.589	-1.34	-0.011	0.129	-1.34	-0.011	0.128	-1.10	-0.010	0.119
11-KRA-11	K-05	3.40	-0.004	4.759	-1.45	-0.009	0.100	-1.33	-0.009	0.098	-1.35	-0.009	0.099
11-KRA-12	K-27	3.82	-0.015	5.347	-0.74	-0.017	0.002	-0.36	-0.015	0.005	-0.50	-0.016	0.004
11-KRA-16	K-40	13.37	-0.036	18.679	-0.11	-0.003	0.023	0.64	-0.010	-0.044	-0.18	-0.002	0.030
11-KRA-17	K-34	9.78	-0.025	13.523	-0.30	-0.015	-0.031	1.03	-0.014	0.048	-0.12	-0.014	-0.020
	IDDP-1				1.13	-0.014	-0.099	1.13	-0.014	-0.099	1.13	-0.014	-0.099
	IDDP-1				0.52	-0.001	0.020	0.52	-0.001	0.020	0.52	-0.001	0.020

4.3 Multiple sulfur isotope model for reservoir sulfate formation in high-temperature geothermal systems

In the Krafla geothermal system, H_2S is the dominant form of sulfur in the fluid at > 230°C accounting for > 80 % on the mole scale of total sulfur in the reservoir fluids, the rest being mostly SO_4. At temperature < 230°C SO_4 becomes increasingly important, accounting for generally 20-55 % on the mole scale of total sulfur in the reservoir fluids. Based on $\delta^{34}S$ of sulfate in minerals, altered rocks and dissolved in the geothermal fluids, Sakai et al. (1980) concluded that majority of sulfate in the Reykjanes geothermal system, SW Iceland, was of seawater origin, but the source fluid in the Reykjanes geothermal system is the surrounding seawater. However, most geothermal systems in Iceland are dilute with meteoric water being the source water (Arnórsson, 1995). The Krafla geothermal system is an example of such system. The source of SO_4 in these systems is, however, unclear.

In order to examine the possible source of SO_4 in the Krafla geothermal system a simple closed system model was constructed in order to investigate the relationship between $\Delta^{33}S$ and $\delta^{34}S$ for H_2S and SO_4 in the fluid. Firstly, it is assumed that all sulfur in the fluid originated from MORB and enters into the geothermal fluids either upon magma degassing or basalt dissolution. Secondly, it is assumed that aqueous SO_4 is produced upon inorganic H_2S oxidation. During closed system H_2S oxidation in a single liquid system, sulfur isotope ratios of the produced sulfate is expressed by (Ono et al., 2012),

$$\delta^{x}SO_4{}^{*} = (H_2\delta^{x}S^{*} + 1)\frac{1-f^{x\alpha}}{1-f} - 1 \quad (11)$$

where $\delta^{x}S^{*}$ is the absolute sulfur isotope ratio for the x=33, 34 and 36 isotope. In the model we further assume insignificant formation of sulfide minerals (e.g., Ohmoto and Goldhaber, 1997). Equation (11) was solved for $\delta^{x}SO_4{}^{*}$ as a function of *f*, i.e. fraction of H_2S oxidized to SO_4 for both sulfur 33 and 34. For these calculations we assumed dissolved sulfide to be present as $H_2S(aq)$. It should be pointed out that almost identical results would have been obtained using the HS^- to SO_4^{2-} fractionation factors. The starting $\delta^{34}S$ and $\Delta^{33}S$ were taken to be within or close to the Icelandic basalts and MORB ratios previously reported (Sakai et al., 1981; Torsander, 1989; Labidi et al., 2012; Ono et al., 2012).

Alternatively, sulfate formation may be related to source water, i.e. meteoric water, and mixing between basalt and meteoric water. The sulfate in meteoric water in Iceland originates predominantly from seawater spray, i.e. it has the same isotope composition as seawater (Gíslason et al., 1996; Gíslason and Torssander, 2006), with values of seawater taken to be $\delta^{34}S$ +21.0 ‰ and $\Delta^{33}S$ +0.050 ‰ (Rees, 1978; Ono et al., 2012). The other end-member is assumed to be basalt with the same sulfur isotope systematics as described above. A simple mixing between basaltic sulfur and seawater sulfate is described according to the equation,

$$\delta^{x}S^{gf} = X^{mw}\delta^{x}S^{mw} + (1-X^{mw})\delta^{x}S^{BAS} \quad (12)$$

where x = 33, 34 and 36, the superscripts gf, mw and BAS denotes geothermal fluid, meteoric water and basalt, respectively, and X^{mw} is the meteoric water mole fraction.

The results of the calculations of multiple sulfur isotope systematics upon H_2S oxidation to SO_4 are compared with the measured values in Figure 14. As observed H_2S in in

the reservoir fluids is identical to those observed in MORB whereas SO_4 in the Krafla fluids shows greater $\delta^{34}S$ values of +2.05 to +13.37 ‰ and more negative $\Delta^{33}S$ -0.036 to -0.004 ‰ compared to H_2S. Such trends may be explained by mass dependent fractionation upon insignificant H_2S ($f > 0.1$) oxidation to SO_4 at temperatures observed in the geothermal reservoir of 200-300°C. On the other hand, possible mixing between meteoric water of seawater origin and sulfur originated from the basalts either through magma degassing or upon basalt dissolution, results in positive $\Delta^{33}S$ with increasing $\delta^{34}S$, a trend not observed for geothermal fluids.

The observed $\Delta^{33}S$ and $\delta^{34}S$ systematics for geothermal fluids at Krafla suggest that the source of sulfides in the fluids is the basaltic magma, either through degassing or upon dissolution of unaltered basalts. At high temperatures, insignificant SO_4 is observed in the fluids but below ~230°C significant concentrations of SO_4 are observed, the source considered to be H_2S oxidation. Sulfate originated from the meteoric source water of the geothermal fluids is considered to be negligible.

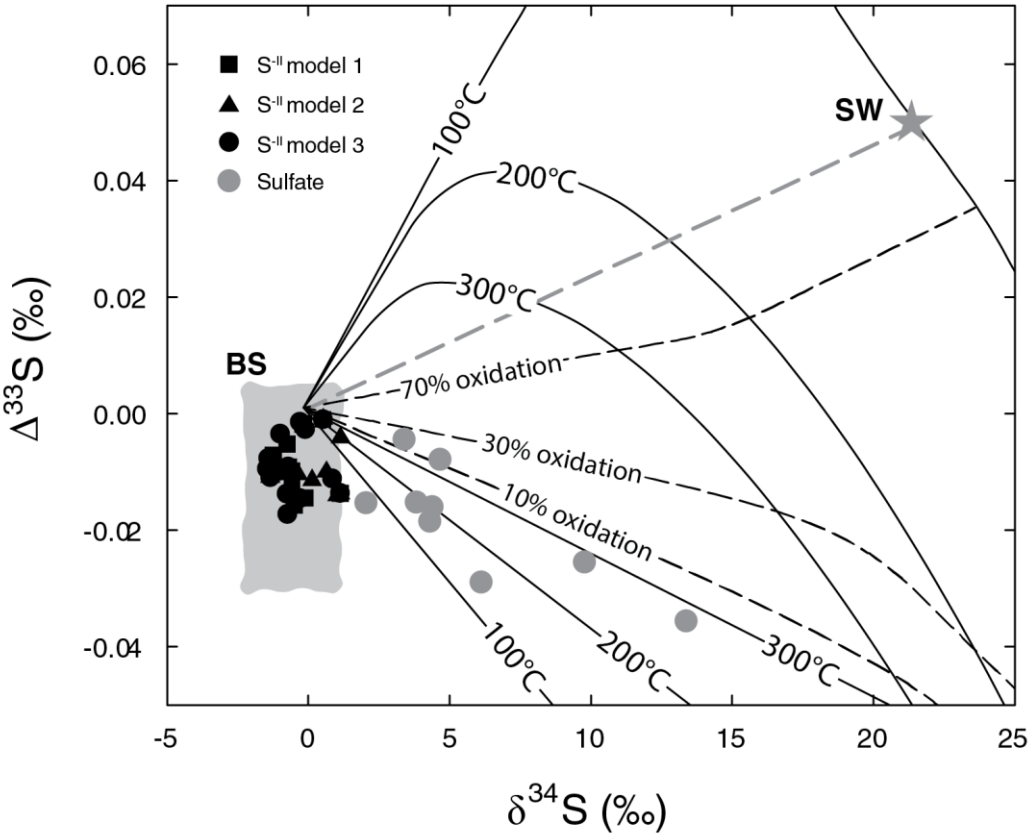

Figure 14 The relationship between $\Delta^{33}S$ and $\delta^{34}S$ sulfide and sulfate in the reservoir fluids at Krafla. The results of the three models for reconstruction of reservoir fluids from data on well fluid discharge are shown (see text). Also shown are the mass dependent fraction between aqueous sulfide and sulfate according to the reaction $H_2S(aq)+4H_2O = \boldsymbol{SO_4^{2-}}(aq) + 2H^+ + 4H_2(aq)$ at 100 to 300°C (solid lines) and at various fractions (f) of H_2S oxidation (conversion) to SO_4. As observed, the heavy $\delta^{34}S$ and negative $\Delta^{33}S$ ratios of sulfate in the reservoir fluids may be explained by moderate oxidation of H_2S at similar temperatures as observed in the reservoir (~200 - 300°C) at Krafla.

5 Summary and conclusions

Multiple sulfur isotope systematics of geothermal fluids at Krafla NE Iceland were studied in order to determine the source and reactions of sulfur in the systems. Fluids from two-phase well discharges and single phase vapor discharges were collected and analysed for major elemental composition, sulfur speciation and multiple sulfur isotopes composition. Based on these, the reservoir fluid composition was assessed using the appropriated model (Arnórsson et al., 2007). The reservoir fluid temperatures ranged from 192 to 437°C with liquid water, vapor and superheated vapor being present in the reservoir. Dissolved sulfide (ΣS^{-II}) and SO_4 predominated in the water phase with trace concentrations of S_2O_3 whereas H_2S was the only species observed in the vapor phase. The sulfur isotope ratios for $\delta^{34}S$ and $\Delta^{33}S$ of sulfide in the reservoir water and vapor are between -1.45 to +1.13 ‰ and -0.017 to -0.001 ‰ whereas $\delta^{34}S$ and $\Delta^{33}S$ of sulfate is significantly different or +3.40 to +13.37 ‰ and -0.036 to 0.000 ‰, respectively. Geochemical modelling was applied to investigate the effects of depressurisation boiling and progressive fluid-rock interaction on the multiple sulfur isotope systematics. Depressurisation boiling upon fluid ascent to the surface results in the liquid phase becoming progressively isotopically lighter both with respect to $\delta^{34}S$ and $\Delta^{33}S$ while the H_2S in the vapor phase become isotopically heavier. This is in accordance with observed well discharge liquid and vapor sulfur isotope ratios. A similar trend occurs upon progressive fluid-rock interaction and pyrite formation, i.e. the liquid water becomes progressively isotopically lighter while the secondary pyrite becomes heavier. The observed $\Delta^{33}S$ and $\delta^{34}S$ systematics for geothermal fluids at Krafla suggest that the source of sulfides in the fluids is the basaltic magma, either through degassing or upon dissolution of unaltered basalts. The same is considered to be the source of SO_4. At high temperatures insignificant SO_4 is observed in the fluids whereas at lower temperature significant concentrations of SO_4 are observed, the source considered to be H_2S oxidation. Sulfate originated from the meteoric source water of the geothermal fluids is considered to be negligible. The findings of the present study indicate that the key parameters influencing multiple sulfur isotope systematics of geothermal fluids under inorganic conditions are two, the isotope composition of the source material or source fluid and sulfur isotope fractionation associated with aqueous and vapor speciation and how these depend and change upon processes occurring in the system including boiling, oxidation and fluid-rock interaction.

References

Alt J. C. and Shanks W. C. (1998) Sulfur in serpentinized oceanic peridotites: serpentinization processes and microbial sulfate reduction. *J. Geophys. Res.* **103**, 9917-9929.

Arnórsson S., Gunnlaugsson E. and Svavarsson H. (1983) The chemistry of geothermal waters in Iceland. II. Mineral equilibria and independent variables controlling water compositions. *Geochim. Cosmochim. Acta* **47**, 547-566.

Arnórsson S. (1995) Geothermal systems in Iceland: Structure and conceptual models—I. High-temperature areas. *Geothermics* **24**, 561-602.

Arnórsson S., Bjarnason J. Ö., Giroud N., Gunnarsson I., Stefánsson A. (2006) Sampling and analysis of geothermal fluids. *Geofluids* **6**, 203–216.

Arnórsson S., Gunnlaugsson E. and Svavarsson H. (1983) The chemistry of geothermal waters in Iceland 2. Mineral equilibria and independent variables controlling water compositions. *Geochim. Cosmochim. Acta* **47**, 547–566.

Arnórsson S., Stefánsson A. and Bjarnason J. Ö. (2007) Fluid–fluid interactions in geothermal systems. *Rev. Min. Geochem.* **65**, 259–312.

Bayon F. E. B. and Ferrer H. (2005) Sulphur isotope ratios in Philippine geothermal systems. In: D'Amore, F. Use of isotope techniques to trace the origin of acidic fluids in geothermal systems, IAEA, Austria, 111-132.

Bjarnason J. Ö. (2010) The chemical speciation program WATCH, version 2.4. ÍSOR – Iceland Geosurvey, Reykjavík, Iceland. Accessible at: http://www.geothermal.is /software .

Czarnacki M. and Halas S. (2012) Ab initio calculations of sulfur isotope fractionation factor for H_2S in aqua-gas system. *Chem. Geol.* **318-319**, 1-5.

Druschel G. K., Schoonen M. A. A., Nordstrom D. K., Ball J. W., Xu Y. and Cohn C. A. (2003) Sulfur geochemistry of hydrothermal waters in Yellowstone National Park, Wyoming, USA. III. An anion-exchange resin technique for sampling and preservation of sulfoxyanions in natural waters. *Geochem. Trans.* **4**, 12–19.

Giggenbach W. F. (1980) Geothermal gas equilibria. *Geochim. Cosmochim. Acta* **44**, 2021–2032.

Giggenbach W. F. (1981) Geothermal mineral equilibria. *Geochim. Cosmochim. Acta* **45**, 393–410.

Giroud N. (2008) A Chemical Study of Arsenic, Boron and Gases in High-Temperature Geothermal Fluids in Iceland. Ph.D. thesis, University of Iceland.

Gíslason S. R. and Torssander P. (2006) Response of sulfate concentration and isotope composition in Icelandic rivers to the decline in global atmospheric SO2 emissions into the North Atlantic Region. *Env. Sci Technol.* **40**, 680-6.

Gíslason S. R., Arnórsson S. and Ármannsson H. (1996) Chemical weathering of basalt in Southwest Iceland; effects of runoff, age of rocks and vegetative/glacial cover. *Amer. J. Sci.* **296**, 837-907.

González-Partida E., Carrillo-Chávez A., Levresse G., Tello-Hinojosa E., Venegas-Salgado S., Ramirez-Silva G., Pal-Verma M., Tritlla J. and Camprubi A. (2005) Hydro-geochemical and isotopic fluid evolution of the Los Azufres geothermal field, Central Mexico. *Appl Geochem* **20**, 23-39.

Gudmundsson B. Th. and Arnórsson S. (2005) Secondary mineral–fluid equilibria in the Krafla and Námafjall geothermal systems, Iceland. *Appl. Geochem.* **20**, 1607–1625.

Gunnarsson I. and Arnórsson S. (2000) Amorphous silica solubility and the thermodynamic properties of H_4SiO_4 in the range of 0 to 350 °C at P_{sat}. *Geochim. Cosmochim. Acta* **64**, 2295–2307.

Gunnlaugsson E. (1977) The origin and distribution of sulphur in fresh and geothermally altered rocks in Iceland. Ph D thesis, University of Leeds, Leeds.

Henley R. W. and Hughes G. O. (2000) Underground fumaroles: "Excess heat" effects in vein formation. *Econ. Geol.* **95**, 453–466.

Horne R. N., Satik C., Mahiya G., Li, K., Ambusso W., Tovar R., Wang C. and Nassori H. (2000) Steam–water relative permeability. World Geothermal Congress. Kyushu-Tohuku, Japan.

Johnson J. W., Oelkers E. H. and Helgeson H. C. (1992) Supcrt92 – a software package for calculating the standard molal thermodynamic properties of minerals, gases, aqueous species, and reactions from 1 bar to 5000 bar and 0°C to 1000°C. *Comput. Geosci.* **18**, 899–947.

Kaasalainen H. and Stefánsson A. (2011a) Chemical analysis of sulfur species in geothermal waters. *Talanta* **85**, 1897-1903.

Kaasalainen H. and Stefánsson A. (2011b) Sulfur speciation in natural hydrothermal waters, Iceland. *Geochim. Cosmochim. Acta* **75**, 2777–2791.

Kamyshny A., Zilberbrand M., Ekeltchik I., Voitsekovski T., Gun J. and Lev O. (2008) Speciation of polysulfides and zerovalent sulfur in sulfide-rich water wells in Southern and Central Israel. *Aquatic Geochemistry* **14**, 171-192.

Labidi J., Cartigny P., Birck J. L., Assayg N. and Bourrand J. J. (2012) Determination of multiple sulfur isotopes in glasses: A reappraisal of the MORB δ34S. *Chem. Geol.* **334**, 189-198.

Li K. and Horne R. N. (2007) Systematic study of steam–water capillary pressure. *Geothermics* **36**, 558–574.

Marini L., Moretti R. and Accornero M. (2011) Sulfur isotopes in magmatic-hydrothermal systems, melts, and magmas. *Rev. Min. Geochem*. **73**, 423-492.

Matsuda K., Shimada K. and Kiyota Y. (2005) Isotope techniques for clarifying origin of SO_4 type acid geothermal-fluid. Case studies of geothermal areas in Kyushu, Japan. *In*: Use of isotope techniques to trace the origin of acidic fluids in geothermal systems. *IAEA-TECDOC-1448*, 83-95.

Ohmoto H. and Goldhaber M. B. (1997) Sulfur and carbon isotopes. *In*: Geochemistry of Hydrothermal Ore Deposits. Barnes H. L. (ed.) J. Wiley and Sons, 517-611.

Ohmoto H. and Rye R. O. (1979) Isotopes of sulfur and carbon. *In*: Geochemistry of Hydrothermal Ore Deposits. Barnes HL (ed) J. Wiley and Sons, 509-567.

Ohmoto H. and Lasaga A. C. (1982) Kinetics of reactions between aqueous sulfates and sulfides in hydrothermal systems. *Geochim. Cosmochim. Acta* **46**, 1727-1745.

Ono S., Keller N. S., Rouxel O. and Alt J. C. (2012) Sulfur-33 constrains on the origin of secondary pyrite in altered oceanic basement. *Geochim. Cosmochim. Acta* **87**, 323-340.

Ono S., Wing B., Johnston D., Farquhar J. and Rumble D. (2006) Mass-dependent fractionation of quadruple stable sulfur isotope system as a new tracer of sulfur biochemical cycles. *Geochim. Cosmochim. Acta* **70**, 2238-2252.

Otake T., Lasaga A. C. and Ohmoto H. (2008) Ab inito calculations for equilibrium fractionations in multiple sulfur isotope systems. *Chem. Geol.* **249**, 357-376.

Parkhurst, D. L. and Appelo, C. A. J., (1999). User's guide to PHREEQC (Version 2)—a computer program for speciation, batch-reaction, one-dimensional transport, and

inverse geochemical calculations. Report 99-4259, U.S. Geological Survey, Water-Resources Investigations.

Pokrovski G. S. and Dubrovinsky L. S. (2011) The S3- ion is stable in geological fluids at elevated temperatures and pressures. *Science* **331**, 1052-1054.

Pritchett J. W. (2005) Dry-steam wellhead discharges from liquid-dominated geothermal reservoirs: a result of coupled nonequilibrium multiphase fluid and heat flow through fractured rock. B. Faybishenko, P.A. Witherspoon, J. Gale (Eds.), Dynamics of Fluids and Transport in Fractured Rock, AGU, Washington, DC, 175–181.

Rees C. E., Jenkins W. J. and Monster J. (1978) The sulfur isotopic composition of ocean water sulfate. *Geochim. Cosmochim. Acta* **42**, 377-382.

Robinson B. W. (1987) Sulphur and sulphate-oxygen isotopes in New Zealand geothermal systems and volcanic discharges. Studies on sulphur isotope variations in nature. Proceedings of an advisory group meeting, Vienna, 17-20 June 1985, IAEA, Vienna, p 31-48.

Sakai H., Gunnlaugsson E., Tómasson J. and Rouse J. E. (1980) Sulfur isotope systematics in Icelandic geothermal systems and influence of seawater circulation at Reykjanes. *Geochim. Cosmochim. Acta* **44**, 1223-1231.

Sakai H. (1983) Sulfur isotope exchange rate between sulfate and sulfide and its application. *Geothermics* **12**, 111-117.

Scott S., Gunnarsson I., Arnórsson S. and Stefánsson A. (2014) Gas chemistry, boiling and phase segregation in a geothermal system, Hellisheidi, Iceland. *Geochim. Cosmochim. Acta* **124**, 170-189.

Sorey M. L., Grant M. A. and Bradford E. (1980) Nonlinear effects in two-phase flow to wells in geothermal reservoirs. *Wat. Res. Res.* **16**, 767–777.

Stefánsson A. and Arnórsson S. (2002) Gas pressures and redox reactions in geothermal fluids in Iceland. *Chem. Geol.* **190**, 251–271.

Stefánsson A., Arnórsson S., Gunnarsson I., Kaasalainen H. and Gunnlaugsson E. (2011) The geochemistry and sequestration of H_2S into the geothermal system at Hellisheidi, Iceland. *J. Volcanol. Geotherm. Res.* **202**, 179-188.

Stefánsson A., Gunnarsson I. and Giroud N. (2007) New methods for the direct determination of dissolved inorganic, organic and total carbon in natural waters by Reagent-Free (TM) Ion Chromatography and inductively coupled plasma atomic emission spectrometry. *Anal. Chim. Acta* **582**, 69–74.

Steinþórsson S. and Sveinbjörnsdóttir Á. E. (1981) Opaque minerals in geothermal well no. 7, Krafla, Northern Iceland. *J. Volcanol. Geotherm. Res.* **10**, 245-261.

Thode H. G., Monster J. and Dunford H. B. (1961) Sulphur isotope geochemistry. *Geochim. Cosmochim. Acta.* **25**. p 159-74.

Torssander P. (1989) Sulfur isotope ratios of Icelandic rocks. *Contrib. Min. Petrol.* **102**, 18-23.

Xu Y., Schoonen M. A. A., Nordstrom D. K., Cunningham K. M. and Ball J. W. (1998) Sulfur geochemistry of hydrothermal waters in Yellowstone National Park: I. The origin of thiosulfate in hot spring waters. *Geochim. Cosmochim. Acta* **62**, 3729–3743.

Xu Y., Schoonen M. A. A., Nordstrom D. K., Cunningham K. M. and Ball J. W. (2000) Sulfur geochemistry of hydrothermal waters in Yellowstone National Park, Wyoming, USA. II. Formation and decomposition of thiosulfate and polythionate in cinder pool. J. *Volcanol. Geotherm. Res.* **97**, 407–423.